

Anisotropic collisional relaxation of the order in atomic angular momenta and related polarization effects during laser excitation

A. G. Petrashen', V. N. Rebane, and T. K. Rebane

St. Petersburg State University, 199164 St. Petersburg
(Submitted 5 January 1993)

Zh. Eksp. Teor. Fiz. **104**, 2610–2643 (August 1993)

A theory is derived for the anisotropic collisional relaxation of the polarization moments of excited atoms in gases and for the numerous polarization effects accompanying this relaxation during excitation by monochromatic laser light. The anisotropy of the distribution function of the relative velocities of the atoms excited by the laser and of the atoms of the surrounding gas mixture is analyzed as a function of the laser frequency and the masses of the particles. Expressions are derived for the rate constants of the anisotropic collisional relaxation of atomic polarization moments in terms of dynamic multipole moments of the velocity distribution function and also in terms of the rate constants of the extremely anisotropic relaxation in oppositely directed monoenergetic beams. Selection rules are found which determine whether dynamic multipole moments of the distribution function participate in a collisional mutual conversion of polarization moments of different ranks. The dynamic quadrupole moment of this function is shown to play a governing role. It is responsible for the most characteristic processes in the anisotropic collisional relaxation. The condition for a transition from anisotropic relaxation to quasi-isotropic relaxation is found. This condition depends on the laser frequency. Calculations are carried out on the collisional conversion of the alignment of atomic angular momenta into their orientation for the particular case of the $2p_4(3p(3/2)_2)$ state of the neon atom and on the onset of an alignment from the level populations for the $3p^2P_{3/2}$ state of the sodium atom. The effect of the alignment of the atomic states and that of the laser frequency on the collisional transfer of populations between atomic levels are studied for the case of the hyperfine levels of the 3P_1 state of the cadmium atom. Transient anisotropic collisional relaxation processes which occur after the excitation of the atoms by the laser pulse lead to beats in the light polarization signals. This polarization beat signal is calculated for the $4p^2P_{3/2}$ state of potassium atoms. Methods for regulating the extent of anisotropy of the relaxation of the polarization moments during laser excitation are discussed.

1. INTRODUCTION

The polarization of the light emitted by excited atoms is determined by the ordering of the angular momenta of the electron clouds of the atoms. The polarization moments ρ_q^κ , which are irreducible spherical tensor components of the density matrix σ_{mm_1} of the ensemble of excited atoms serve as qualitative and also quantitative characteristics of this ordering. Their ranks κ take on integer values from 0 to $2J$, where J is the quantum number of the angular momentum of the given atomic state; their projections onto the quantization axis (q) take on values from $-\kappa$ to $+\kappa$. D'yakonov, Perel', and Omont¹⁻³ were the first investigators to reach a clear understanding that the description of all possible types of order of the atomic angular momenta reduces to the specification of polarization moments and that the polarization of the emitted light (linear, circular, or, in general, elliptical) is determined completely by these polarization moments. It follows from the selection rules for dipole radiation that the linear polarization of the light is determined by five independent components of the second-rank polarization moment ρ_q^2 (also called the alignment tensor), while the circular polarization is determined

by three independent components of the first-rank polarization moment ρ_q^1 (the orientation vector).

Atomic collisions alter the states of the excited atoms. In particular, the ordering of their angular momenta changes. These changes lead to collisional relaxation of the polarization moments and thus to a change in the light polarization observed experimentally. This fact underlies polarization-spectroscopy methods for studying the effect of collisions on the internal state of atomic particles. These methods, combined with quantum collisions theory, constitute a rapidly developing branch of modern optics. The work in this field is reviewed in Refs. 4–7.

Starting with the fundamental studies by Perel', D'yakonov, and Omont,¹⁻³ research on the effect of collisions on the ordering of atomic angular momenta and on the polarization of light has been carried out for the case of random collisions, in the course of which the directions of the particle collisions are distributed at random (isotropically). In this isotropic case, the resultant effect of collisions on the density matrix of the excited atoms is spherically symmetric, and all the polarization moments ρ_q^κ decay independently, with rate constants which depend on their ranks κ but not on their projections q . This circumstance leads in particular to differences in the rates of collisional disrup-

tion of the alignment and orientation, i.e., of the linear and circular polarizations of the light.^{2,3}

The mechanism for the collisional relaxation of the ordering of the angular momenta of excited atoms becomes considerably more complicated in the anisotropic case, in which the velocity distribution of the colliding particles has a special direction. This circumstance was first pointed out in papers by one of the present authors^{8,9} and, independently, by Lombardi.¹⁰ The anisotropic collisional relaxation has a number of interesting features, which distinguish substantially from isotropic relaxation. While isotropic relaxation simply leads to collisional disruption of all types of order of the atomic angular momenta and suppresses the associated polarizations of the light, anisotropic relaxation also has a constructive effect, which creates order. It leads to mutual conversions of the various types of order and to the appearance of new types of order of atomic angular momenta. In a sense, anisotropic collisional relaxation transfers anisotropy from the particle velocity distribution to the angular-momentum distribution of the electron clouds of the particles.¹¹

Distinctive features of anisotropic collisional relaxation follow from simple but rigorous symmetry considerations. As has already been mentioned, the ordering of the angular momenta of the electron clouds of the atoms is determined by the polarization moments, which are found by expanding the density matrix of the ensemble of atoms, σ_{mm_1} , in terms of irreducible representations of the 3D rotation group:

$$\rho_q^\kappa = \sum_{mm_1} (-1)^{J-m_1} \begin{bmatrix} J & J & \kappa \\ m & -m_1 & q \end{bmatrix} \sigma_{mm_1}. \quad (1)$$

The square brackets denote the Clebsch–Gordan coefficients,¹² and m and m_1 are the magnetic quantum numbers of atoms in an electronic state with an angular momentum J .

For isotropic collisions, all particle-collision direction are equiprobable, so the net effect of collisions on the density matrix of the ensemble of atoms has spherical symmetry. Isotropic collisions thus alter neither the rank κ nor the projection q of the polarization moment. All the polarization moments decay under the influence of these collisions in accordance with simple single-exponential laws determined by the differential equations

$$\frac{d}{dt} \rho_q^\kappa = -\gamma^\kappa \rho_q^\kappa. \quad (2)$$

The constants of the isotropic collisional relaxation, γ^κ , which appear in these equations are positive. They depend on the rank κ of the polarization moment, but not on its projection q . It can also be seen from (2) that under isotropic conditions there is no collisional mutual conversion of the polarization moments of different ranks κ (or with different projections onto the quantization axis, q).

Under anisotropic conditions, the resultant effect of collisions on the ensemble of atoms does not have spherical symmetry; it has only axial symmetry, with respect to the special spatial direction along which the collisions of par-

ticles occur most frequently (or most rarely). Accordingly, the collisional relaxation of the polarization moments is currently classified in terms of irreducible representations of the $C_{\infty v}$ group, which contains rotations through arbitrary angles around the anisotropy axis and mirror reflections in planes passing through this axis. As a result, the anisotropic collisional relaxation of the polarization moments of the ensemble of excited atoms of species A in a gaseous medium of atoms of species B is described by the equations

$$\frac{d}{dt} \rho_q^\kappa = -n_B \sum_{\kappa_1} \langle v \sigma_q^{\kappa \kappa_1} \rangle \rho_q^{\kappa_1}. \quad (3)$$

Here n_B is the number density of the atoms of gas B. The matrix of rate constants of the anisotropic collisional relaxation, $\langle v \sigma_q^{\kappa \kappa_1} \rangle$, on the right side of this equation is diagonal with respect to the projections q of the polarization moments, but not with respect to their ranks κ and κ_1 . Anisotropic collisions thus “mix” the polarization moments of different ranks but conserve their projections onto the anisotropy axis. A more detailed examination of the symmetry properties shows that if the projections of the polarization moments onto the anisotropy axis are non-zero (if $q \neq 0$) collisional mutual conversion of the polarization moments of arbitrary ranks κ and κ_1 occurs. If these projections are instead zero ($q = 0$), only those moments whose ranks κ and κ_1 have the same parity undergo mutual conversion.

The picture of the polarization-moment relaxation of the ensemble of atoms is thus rendered more complicated by anisotropic collisions. This added complexity leads to an entire new class of polarization effects, which are impossible in principle under isotropic conditions. Among them are collisional conversion of alignment into orientation, accompanied by a transition from linear polarization of the light to circular polarization;^{8–10,13–22} collisional generation of a longitudinal component ρ_0^2 of the alignment of the atomic angular momenta along the anisotropy axis and the appearance of a corresponding linear polarization of the light;^{23–32} the appearance of a dependence of the rate of the collisional depolarization of the light on the direction of the polarization vector with respect to the anisotropy axis;^{33–35} the important effect of light polarization on the probabilities for collisional transitions between atomic levels;^{36–45} and transient polarization-beat processes due to the joint collisional relaxation of polarization moments of various ranks.^{46–49}

We thus see that the anisotropic collisional relaxation of the order of the angular momenta of the excited atoms is characterized by diverse processes of mutual conversion and generation of polarization moments and that it is accompanied by a rich variety of interesting polarization-spectroscopy effects.

One of the most promising methods for experimentally studying such effects is to use monochromatic laser light.⁴ The laser light plays two roles in this process: While exciting the atoms of interest, it also performs a selection of these atoms in terms of their velocity along the laser beam.

Tuning the laser frequency within the Doppler profile of the spectral line makes it possible to create an ensemble of excited atoms with an adjustable velocity-distribution anisotropy in this case. It thus becomes possible to carry out a detailed study of the various processes which occur in the course of anisotropic collisions.

In this paper we are interested in the anisotropic collisional relaxation of states of excited atoms in gases and in the polarization effects accompanying this relaxation under conditions of monochromatic laser excitation. In the first few sections of this paper we present a theory of anisotropic relaxation. We then apply it to the most characteristic polarization-spectroscopy manifestations of changes in the order of atomic angular momenta due to anisotropic collisions.

2. VELOCITY DISTRIBUTION OF COLLIDING PARTICLES DURING LASER EXCITATION

We consider a gaseous mixture of atoms of two species, A and B with masses M_A and M_B , at a temperature T . The number density of the A atoms is low in comparison with that of the B atoms: $n_A \ll n_B$. We assume that the velocities of the B atoms and of the unexcited A atoms have Maxwellian distributions. We assume that a monochromatic laser beam of frequency ν , directed along the z axis, excites the A atoms within the Doppler profile of some spectral line, which is centered at the frequency ν_0 . The laser light is then absorbed exclusively by those A atoms for which the z projection of the velocity is

$$v_0 = c(\nu - \nu_0) / \nu_0 \quad (4)$$

and depends on the detuning of the laser frequency ν from the center of the Doppler profile, ν_0 . As a result of the absorption of the light, an ensemble of excited A atoms with a strictly fixed z velocity component arises. The velocity distribution of this ensemble is

$$f(\mathbf{v}_A) = \frac{M_A}{2\pi kT} \exp\left[-\frac{M_A}{2kT}(v_{Ax}^2 + v_{Ay}^2)\right] \delta(v_{Az} - v_0). \quad (5)$$

By virtue of the condition $n_A \ll n_B$, the relaxation of the states of the excited A atoms is determined by their collisions with atoms of the background gas B. It follows from the Maxwellian velocity distribution of the B atoms and from distribution (5) for the velocities of the excited A atoms that the distribution of their relative velocities $\mathbf{v} = \mathbf{v}_B - \mathbf{v}_A$ is described by

$$\mathcal{F}(\mathbf{v}) = \frac{M_A}{M_A + M_B} \left(\frac{M_B}{2kT}\right)^{3/2} \times \exp\left[-\frac{M_A M_B (v_x^2 + v_y^2)}{2(M_A + M_B)kT} - \frac{M_B (v_z - v_0)^2}{2kT}\right]. \quad (6)$$

This distribution is Maxwellian [corresponding to particles with masses equal to the reduced mass of the A and B atoms, i.e., $M_A M_B / (M_A + M_B)$] in directions perpendicular to the laser beam. Along the beam, this distribution is a

Maxwellian distribution shifted along the z axis in velocity space to the point $v_x = v_y = 0$, $v_z = v_0$, for particles with masses M_B . The distribution function (6) is determined entirely by specifying the three quantities v_0 , kT/M_A , and kT/M_B . The last of these can conveniently be replaced by the two dimensionless parameters¹⁴

$$\xi = v_0 \sqrt{\frac{M_A}{2kT}}, \quad \eta = \frac{M_B}{M_A + M_B}. \quad (7)$$

The velocity distribution (6) can then be written

$$\mathcal{F}(\mathbf{v}) = \left(\frac{\xi}{v_0}\right)^3 \left(\frac{\eta^3}{\pi^3(1-\eta)}\right)^{1/2} \times \exp\left[-\frac{\xi^2 \eta}{v_0} \left[v_x^2 + v_y^2 + \frac{(v_z - v_0)^2}{1-\eta}\right]\right]. \quad (8)$$

This distribution has a constant value on the surfaces

$$v_x^2 + v_y^2 + \frac{(v_z - v_0)^2}{1-\eta} = \text{const.} \quad (9)$$

In the space of the relative velocity \mathbf{v} , these surfaces are ellipsoids of revolution, similar to each other, with a common center at the point $v_x = v_y = 0$, $v_z = v_0$. These ellipsoids are oblate along the z axis and have a minor-to-major semi-axis ratio

$$\sqrt{1-\eta} = \sqrt{M_A / (M_A + M_B)}. \quad (10)$$

In the limit of an "infinitely light" impurity gas B ($M_B \ll M_A$), the parameter η tends toward zero, and the ellipsoids in (9) become spheres. At the same time, the coefficients of the expression in square brackets in the exponential function in (8) tend toward zero. The meaning is that anisotropic velocity distribution (8) tends toward an isotropic (and infinitely diffuse) Maxwellian distribution in this limiting case. For $\eta \neq 0$, i.e., for nonzero masses of the A and B particles, the velocity distribution in (8) is always anisotropic, and the deviation of the ellipsoids in (9) from spheres increases with increasing η , i.e., with increasing mass ratio M_B/M_A . In the limit of an "infinitely heavy" background gas B ($M_B \gg M_A$), the parameter η tends toward one, and ellipsoids (9) become thin disks whose planes are perpendicular to the laser beam. For arbitrary values of the masses of the A and B particles, the common center of all the ellipsoids in (9) can be adjusted by tuning the laser frequency, which determines v_0 in accordance with (4).

Figure 1 shows intersections of the ellipsoids of constant values of the velocity distribution function as determined by (9) and the xz plane for certain characteristic values of η and v_0 . A common characteristic of the anisotropy of the velocity distribution can be found by comparing the mean square velocities along the coordinate axes calculated with the help of this distribution. For distribution (8), these mean square velocities are

$$\overline{v_x^2} = \overline{v_y^2} = \frac{v_0^2}{2\xi^2 \eta}, \quad \overline{v_z^2} = v_0^2 \left(1 + \frac{1-n}{2\xi^2 \eta}\right). \quad (11)$$

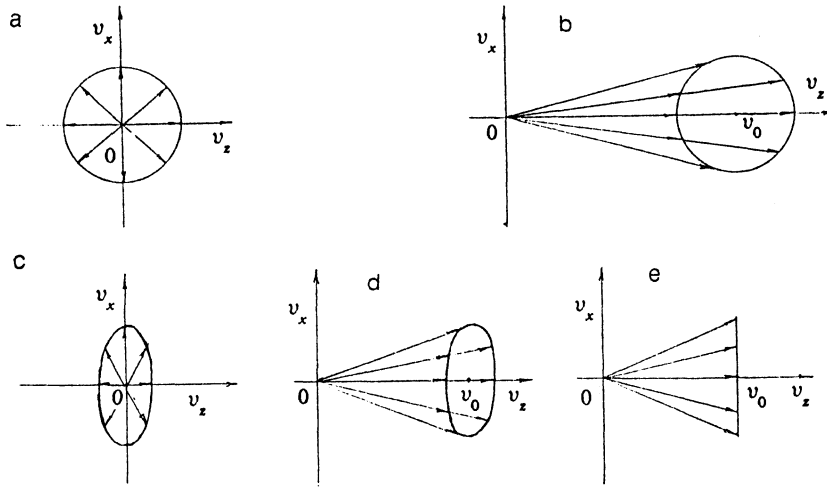


FIG. 1. Contour surfaces of the distribution function of the relative velocities of laser-excited atoms A and background-gas atoms B. a: Zero detuning of the laser frequency and “infinitely light” background gas ($\Delta\nu=0$, $M_B \ll M_A$). The distribution of relative velocities is isotropic and “infinitely diffuse.” b: Nonzero detuning of the laser frequency and “infinitely light” background gas ($\Delta\nu \neq 0$, $M_B \ll M_A$). The distribution of relative velocities is an isotropic, “infinitely diffuse” distribution shifted along the z axis. c: Zero detuning of the laser frequency and finite masses of the A and B particles ($\Delta\nu=0$, $M_B/M_A=2.5$). d: Nonzero detuning of the laser frequency and finite masses of the particles ($\Delta\nu \neq 0$, $M_B/M_A=2.5$). e: Nonzero detuning of the laser frequency and “infinitely light” test gas A ($\Delta\nu \neq 0$, $M_B \gg M_A$). All the vector relative velocities of the A and B particles have the same z component, equal to v_0 .

We take the degree of anisotropy of the distribution function to be the difference between the mean square values of the relative velocities of the A and B particles along the laser beam and in a direction transverse to this beam, divided by the mean square value of their total relative velocity:

$$\gamma = \frac{\overline{v_z^2} - \overline{v_x^2}}{\overline{v_x^2} + \overline{v_y^2} + \overline{v_z^2}} = \frac{(2\xi^2 - 1)\eta}{(2\xi^2 - 1)\eta + 3}. \quad (12)$$

The degree of anisotropy lies in the interval $-0.5 \leq \gamma \leq 1$. It reaches its lower limit with $\xi=0$ and $\eta=1$ and its upper limit when, for an arbitrary nonzero η , the value of ξ goes off to $\pm\infty$.

It can be seen from (12) that the degree of anisotropy increases monotonically with increasing absolute value of the parameter ξ [and of the detuning of the laser frequency from the center of the Doppler profile, which is related to the parameter ξ by Eqs. (4) and (7)]. At the points $\xi = \pm\sqrt{1/2} = 0.71$, it crosses zero and tends toward one on the far wings of the Doppler profile (at $\xi = \pm\infty$). The points $\xi = \pm 0.71$ can be called “quasi-isotropy points.”⁵⁰ At these points, which are separated from the center of the Doppler line by a distance equal to $\pm 84\%$ of the half-width of the Doppler profile, the mean square relative velocities of the A and B particles are identical along all three coordinate axes, and distribution (8) is in a sense reminiscent of an isotropic velocity distribution. Near the quasi-isotropy points, the anisotropic nature of the collisional relaxation is muted; in particular, the collisional mutual conversion of the polarization moments of different ranks disappears. When the absolute value of ξ is less than (or, correspondingly, greater than) 0.71, collisions of excited A atoms with B particles in directions perpendicular to (or, correspondingly, parallel to) the laser beam are predominant. The degree of anisotropy of the relaxation can thus be adjusted easily by varying the laser frequency; it increases as the laser frequency deviates in either direction from the quasi-isotropy points.

Yet another useful result follows from (12): We see from this formula that the absolute value of the degree of

anisotropy γ increases monotonically with increasing value of the parameter η , i.e., the mass ratio M_B/M_A . Accordingly, the best way to impose anisotropy on the distribution of relative velocities of the colliding particles and to create conditions for anisotropic collisional relaxation is to use a heavy background gas B—a heavy inert gas or chemically stable polyatomic molecules.

3. RATE CONSTANTS OF THE ANISOTROPIC COLLISIONAL RELAXATION OF ATOMIC POLARIZATION MOMENTS DURING LASER EXCITATION

Since the z axis (the direction of the laser beam) is the anisotropy axis of velocity distribution (8), the collisional relaxation of the polarization moments of the excited A atoms is described by the differential equations (3). These equations have collisional-relaxation rate constants $\langle v\sigma_q^{\kappa\kappa_1} \rangle$ which are not only diagonal but also off-diagonal in terms of the ranks κ and κ_1 of the polarization moments. We turn now to a calculation of these rate constants.

We first consider the extremely anisotropic case of collisions of atoms A and B in oppositely directed monoenergetic beams, in the course of which their relative velocity has a strictly fixed value v and is directed parallel to the z axis. In this case the effective cross sections for collisional relaxation, $\sigma_q^{\kappa\kappa_1}(v)$, of the polarization moments can be calculated directly by solving, by the impact-parameter method, the system of differential equations describing the change in the state of excited atom A in the course of a collision with a particle B. We have carried out corresponding numerical calculations for the case of rectilinear particle trajectories, for a power-law splitting of a degenerate energy level of an A atom with an angular momentum J in the field of an incident particle B, at a distance R :

$$E_{Jm}(R) = \frac{3m^2 - J(J+1) \Delta C}{3[J][J+1/2] R^n}. \quad (13)$$

The square brackets denote the greatest integer, and m is the projection of the angular momentum of the A atom onto the A–B direction. If the A and B particles are neutral, we have $n=6$, and the value of ΔC is determined by

their dispersive interaction. In the case of a collision of an A particle with a B ion we have $n=3$, and ΔC is determined by the orientational energy of the quadrupole moment of the A atom in the electric field of this ion.

For both interaction laws ($n=6$ and $n=3$), and for angular momenta $J=1, 3/2$, and 2 of the excited A atom, we integrated the system of differential equations numerically by the impact-parameter method. We used a large number (500) of individual particle trajectories differing in impact parameter. For each trajectory we then constructed a bilinear combination of scattering matrix elements which determines the contribution of the given individual collision to the increments in the polarization moments of the A atom. We then averaged the results over the impact parameter. The values found for the effective cross sections $\sigma_q^{\kappa\kappa_1}$ through these calculations for the anisotropic collisional relaxation of the polarization moments are tabulated in Ref. 41. They can be described by

$$\sigma_q^{\kappa\kappa_1}(v) = a_q^{\kappa\kappa_1} \left| \frac{\Delta C}{\hbar v} \right|^{2/(n-1)}, \quad (14)$$

where $a_q^{\kappa\kappa_1}$ are dimensionless numbers, and the additional factor $|\Delta C/\hbar v|^{2/(n-1)}$ has the dimensionality of a square length. The effective cross sections in (14) are power-law functions of the relative velocity of the colliding particles, v . The rate constants for the collisional relaxation of the polarization moments in this extremely anisotropic case of monoenergetic collisions along the z axis are

$$v\sigma_q^{\kappa\kappa_1}(v) = a_q^{\kappa\kappa_1} \left| \frac{\Delta C}{\hbar} \right|^{2/(n-1)} v^{(n-3)/(n-1)}. \quad (15)$$

To find the rate constants $\langle v\sigma_q^{\kappa\kappa_1} \rangle$ for the relaxation of the polarization moments in the case of a real, partially anisotropic velocity distribution (8), we imagine the collisional relaxation to be a superposition of an infinite number of extremely anisotropic relaxations corresponding to monoenergetic collisions with velocities v along all possible directions, weighted by $\mathcal{F}(\mathbf{v})$. As a result we find the following expression for the rate constants of interest in Eqs. (3):

$$\langle v\sigma_q^{\kappa\kappa_1} \rangle = \sum_{q_1} \int D_{qq_1}^{\kappa}(\varphi\theta\psi) D_{qq_1}^{\kappa_1}(\varphi,\theta,\psi) \times \mathcal{F}(\mathbf{v}) \sigma_{q_1}^{\kappa\kappa_1}(v) v^3 \sin\theta d\theta d\varphi d\psi, \quad (16)$$

where the D are the Wigner functions. The polar angle θ is reckoned from the anisotropy axis (from the laser beam). Substituting (15) into (16) and integrating over the angle ψ , we find

$$\langle v\sigma_q^{\kappa\kappa_1} \rangle = \left| \frac{\Delta C}{\hbar} \right|^{2/(n-1)} \sum_{l_1} (-1)^{q+q_1} \begin{bmatrix} \kappa & \kappa_1 & l \\ q & -q & 0 \end{bmatrix} \times \begin{bmatrix} \kappa & \kappa_1 & l \\ q_1 & -q_1 & 0 \end{bmatrix} a_{q_1}^{\kappa\kappa_1} \int \mathcal{F}(\mathbf{v}) P_l(\cos\theta) \times \sigma_{q_1}^{\kappa\kappa_1}(v) v^{2+(n-3)/(n-1)} dv \sin\theta d\theta d\varphi. \quad (17)$$

The matrix of coefficients $a_q^{\kappa\kappa_1}$ in (14) has several useful symmetry properties.^{51,52} In particular, it follows from the symmetry of the collision with respect to the plane containing the vector relative velocity that we have

$$a_q^{\kappa\kappa_1} = (-1)^{\kappa-\kappa_1} a_{-q}^{\kappa\kappa_1}. \quad (18)$$

Making use of the symmetry properties of the Clebsch-Gordan coefficients, we then conclude that only terms with even values of l are retained in the sum (17).

Taking its axial symmetry into account, we see that the velocity distribution in (8) has the following expansion in Legendre polynomials:

$$\mathcal{F}(\mathbf{v}) = \sum_{l=0}^{\infty} f_l(v) P_l(\cos\theta). \quad (19)$$

The coefficients of this expansion are

$$f_l(v) = \frac{2l+1}{4\pi} \int \mathcal{F}(\mathbf{v}) P_l(\cos\theta) \sin\theta d\theta d\varphi. \quad (20)$$

Substituting (19) into (17), and integrating over angles, we find the following expressions for the rate constants for the relaxation of the polarization moments under real conditions, with partially anisotropic collisions:

$$\langle v\sigma_q^{\kappa\kappa_1} \rangle = \left| \frac{\Delta C}{\hbar} \right|^{2/(n-1)} \sum_{l_1} (-1)^{q+q_1} \begin{bmatrix} \kappa & \kappa_1 & 2l \\ q & -q & 0 \end{bmatrix} \times \begin{bmatrix} \kappa & \kappa_1 & 2l \\ q_1 & -q_1 & 0 \end{bmatrix} a_q^{\kappa\kappa_1} \times \frac{4\pi}{2l+1} \int f_{2l}(v) v^{2+(n-3)/(n-1)} dv. \quad (21)$$

4. DYNAMIC MULTIPOLE MOMENTS OF THE VELOCITY DISTRIBUTION

The result derived in the preceding section of this paper for the rate constants for anisotropic collisional relaxation can be written in a more compact form. To do this, we introduce dimensionless quantities, "dynamic multipole moments" of the distribution function of the relative velocities of the colliding particles:

$$S_{2l}^{(\xi)} = \frac{4\pi}{2l+1} \left[\frac{M_A M_B}{2(M_A + M_B)} \right]^{\xi/2} \int_0^{\infty} f_{2l}(v) v^{2+\xi} dv. \quad (22)$$

These dynamic multipole moments are (within a constant factor) integrals of even coefficients (20) in the expansion of the velocity distribution, calculated with a weight $v^{2+\xi}$, where

$$\xi = (n-3)/(n-1) \quad (23)$$

is determined by dynamic law (13) for the splitting of the degenerate energy level of excited A atom in the field of particle B.

Substituting the explicit expression for velocity distribution (8) into (20), and then substituting the result into (22), we find

$$S_{2l}^{(\xi)}(\xi, \eta) = \frac{2}{\sqrt{\pi(1-\eta)}} \int_0^\infty t^{2+\xi} dt \int_{-1}^{+1} \times \exp \left[-t^2(1-u^2) - \frac{(tu - \xi \sqrt{\eta})^2}{1-\eta} \right] \times P_{2l}(u) du. \quad (24)$$

We see that the dynamic multipole moments of the velocity distribution depend on the exponent ξ [see (23)] in the law describing the interaction of the colliding particles; they also depend on the detuning of the laser frequency and the temperature and masses of the particles, through the parameters ξ and η in (7).

The integrals in (24) cannot be evaluated in closed form, but they can be represented by rapidly converging series containing the gamma function and the incomplete gamma function. We then find the following formula for the dynamic multipole moments of the distribution function:

$$S_{2l}^{(\xi)}(\xi, \eta) = \exp(\xi^2) (1+\eta)^{1+\xi/2} \left(\frac{\eta}{4}\right)^l \times \sum_{m=0}^l \left(\frac{\xi^2}{1-\eta}\right)^{l-m} \frac{(-1)^m (4l-2m)!}{m!(2l-m)!(2l-2m)!} \times \sum_{k=0}^\infty \frac{\Gamma(k+(2l+\xi+3)/2)}{k! \Gamma(k+2l+3/2)} \times \eta^k \Gamma\left(k+m+1, \frac{\xi^2}{1-\eta}\right). \quad (25)$$

Using (22), we can put expression (21), for the rate constants for the collisional relaxation of the polarization moments, in the following form:

$$\langle v \sigma_q^{\kappa \kappa_1} \rangle = g_n \sum_{q_1} (-1)^{q+q_1} \begin{bmatrix} \kappa & \kappa_1 & 2l \\ q & -q & 0 \end{bmatrix} \times \begin{bmatrix} \kappa & \kappa_1 & 2l \\ q_1 & -q_1 & 0 \end{bmatrix} a_{q_1}^{\kappa \kappa_1} \cdot S_{2l}^{(\xi)}(\xi, \eta). \quad (26)$$

The coefficient of the summation,

$$g_n = \left| \frac{\Delta C}{\hbar} \right|^{2/(n-1)} \left[\frac{2(M_A + M_B)kT}{M_A M_B} \right]^{(n-3)/2(n-1)}, \quad (27)$$

has the dimensionality of a rate constant ($\text{cm}^{-3} \cdot \text{s}^{-1}$). The value of this coefficient is determined by the splitting of the given level of the A atom in the field of the B particle [see (13)], by the reduced mass of the A and B particles, and by the temperature.

Expression (26), along with Eqs. (3), constitutes the law of the anisotropic collisional relaxation of the atomic polarization moments for the case of monochromatic laser excitation. In addition to the Clebsch–Gordan coefficients, which describe the kinematics of the summation of the angular momenta, this law includes the coefficients $a_q^{\kappa \kappa_1}$, which determine the effective cross sections for collisional relaxation in the extremely anisotropic monoenergetic case [see (14)] and the dynamic multipole moments of the velocity distribution, $S_{2l}^{(\xi)}(\xi, \eta)$.

The triangle inequality for the Clebsch–Gordan coefficients in the sum (26) imposes a requirement which severely limits the ranks of the dynamic multipole moments which determine the rate constants for the relaxation of the polarization moments:

$$|\kappa - \kappa_1| \leq 2l \leq \kappa + \kappa_1. \quad (28)$$

Since the polarization-moment ranks κ and κ_1 can take on integer values from 0 to $2J$ for an electronic state with a given angular momentum, it follows from (28) that the anisotropic collisional relaxation is governed by a small number of dynamic multipole moments of the velocity distribution function. For the case in which the electron angular momentum of the excited state is $J=1$, for example, the collisional relaxation is governed completely by the three dynamic multipole moments with ranks $2l=0, 2$, and 4 ; in the case $J=3/2$, it is governed by the four moments with ranks $2l=0, 2, 4$, and 6 ; for $J=2$, it is governed by the five moments with $2l=0, 2, 4, 6$, and 8 ; etc.

Note that any relative-velocity distribution for which all the even dynamic multipole moments S_{2l} are zero for $l \geq 1$, but for which the odd dynamic multipole moments S_{2l+1} can have arbitrary values, is indistinguishable from an isotropic distribution function in terms of the properties of the collisional relaxation of the polarization moments. In the case of such a distribution function, the sum in (26) contains only a single term ($l=0$). From the properties of the Clebsch–Gordan coefficients we then find the selection rule $\kappa = \kappa_1$. As a result, the matrix of rate constants for the collisional relaxation of the polarization moments turns out to be diagonal in κ , and its elements are independent of q . The axisymmetric relaxation law (3) then converts into isotropic relaxation law (2), in which the relaxation constants are given by

$$\gamma^\kappa = \frac{n_B g_n S_0^{(\xi)}(\xi, \eta)}{(2\kappa+1)} \sum_{q_1} a_{q_1}^{\kappa \kappa}. \quad (29)$$

We thus see that the symmetry properties of collisional process (18), which leads to the disappearance of the odd terms in sum (17), is of fundamental importance in the theory of the anisotropic collisional relaxation of polarization moments.

5. COLLISIONAL MUTUAL CONVERSION OF POLARIZATION MOMENTS; CONVERSION OF AN ANISOTROPIC RELAXATION INTO A QUASI-ISOTROPIC RELAXATION

Let us discuss the role played by dynamic multipole moments of the velocity distribution function in the collisional mutual conversion of the polarization moments of an ensemble of excited atoms.

Mutual conversion of the polarization moments of rank κ and κ_1 is possible if the rate constant $\langle v \sigma_q^{\kappa \kappa_1} \rangle$ given by (26) is nonzero. For this condition to hold, at least one product of Clebsch–Gordan coefficients on the right side of this equation must be nonzero. We are thus led to condition (28), which relates the ranks of the jointly relaxing polarization moments κ and κ_1 and which brings about this relaxation of the dynamic multipole moments $S_{2l}^{(\xi)}$. In

TABLE I. Participation of the dynamic multipole moments of the distribution function of the relative velocities of the colliding particles in the relaxation and mutual conversion of the polarization moments of the excited atoms.

$\kappa \backslash \kappa_1$	0	1	2	3	4
0	S_0	—	S_2	—	S_4
1	—	S_0, S_2	S_2	S_2, S_4	S_4
2	S_2	S_2	S_0, S_2, S_4	S_2, S_4	S_2, S_4, S_6
3	—	S_2, S_4	S_2, S_4	S_0, S_2, S_4, S_6	S_2, S_4, S_6
4	S_4	S_4	S_2, S_4, S_6	S_2, S_4, S_6	S_0, S_2, S_4, S_6, S_8

Note. The diagonal cells of this table ($\kappa_1 = \kappa$) contain the dynamic multipole moments which determine the relaxation of the polarization moment of rank κ , while the off-diagonal cells ($\kappa_1 \neq \kappa$) contain the multipole moments which determine the mutual conversion of the polarization moments of ranks κ and κ_1 .

particular, the collisional mutual conversion of the alignment ($\kappa=2$) and orientation ($\kappa_1=1$), like the collisional creation of an alignment ($\kappa=2$) from the populations of atomic levels ($\kappa_1=0$), is determined by the sole quantity $S_2^{(\xi, \eta)}$, i.e., by the dynamic quadrupole moment of the velocity distribution function. The dynamic quadrupole moment of this function is thus the cause of the most characteristic anisotropic-relaxation processes. Higher-order even dynamic multipole moments $S_{2l}^{(\xi)}$ with ranks $2l=4, 6, \dots$ are manifested in the collisional mutual conversion of the polarization moments of higher ranks κ , including the octupole orientation ($\kappa=3$), the hexadecupole alignment ($\kappa=4$), and even higher analogs of the orientation (with $\kappa=2^{2l+1}$) and the alignment (with $\kappa=2^{2l}$).

These ideas are explained clearly by Table I. The cells of this table contain the dynamic multipole moments S_{2l} which are responsible for the collisional relaxation and for the mutual conversion of the polarization moments of ranks κ and κ_1 . This table covers atomic states with angular momenta $J=1, 3/2$, and 2, so the ranks of the polarization moments, κ and κ_1 , range from 0 to 4.

Occupying an important place among the dynamic multipole moments of the velocity distribution is the dynamic quadrupole moment. This moment completely determines the collisional creation of an alignment from the populations ($\kappa=2, \kappa_1=0$) and the conversion of an align-

ment into an orientation ($\kappa=1, \kappa_1=2$). How does this moment depend on the parameters ξ and η in (7), which characterize the distribution function of the relative velocities of the colliding particles? Figure 2 shows the results of a calculation of this dependence through a summation of the infinite series in (25), for the case in which excited atoms of species A collide with neutral atoms of the background gas B ($\eta=6, \xi=3/5$).

The abscissa ($\eta=0$) in this figure corresponds to a completely isotropic velocity distribution and to a zero value of S_2 . As we move from the origin of coordinates ($\xi=\eta=0$) along the η axis, the quantity S_2 goes negative, and at the point $\xi=0, \eta=1$ it reaches the value -0.45 . As the parameter ξ is raised (i.e., as the detuning of the laser frequency from the center of the Doppler profile increases), S_2 increases, going from negative values to positive. The boundary between the regions of its negative and positive values, found from the equation

$$S_2(\xi, \eta) = 0, \quad (30)$$

corresponds to a quasi-isotropic collisional relaxation, since the collisional conversion of an alignment into an orientation and the collisional creation of an alignment from populations disappear at this boundary. The absolute value of the dynamic quadrupole moment of the relative-

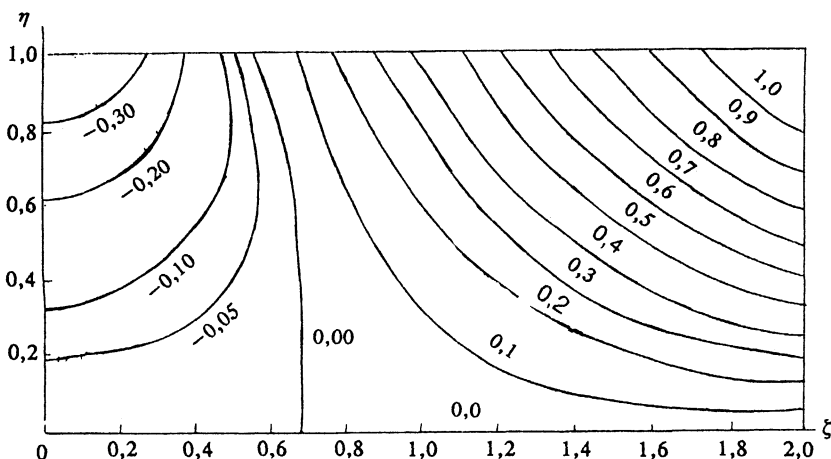


FIG. 2. Dynamic quadrupole moment of the distribution function of the relative velocities of laser-excited atoms A and background-gas atoms B in the case of a dispersive A-B interaction of the $1/R^6$ type as a function of the dimensionless parameters ξ and η [see (7)]. The dynamic quadrupole moment is zero at the abscissa (for $J=0$) and also on the nearly vertical curved line separating the regions of its negative and positive values.

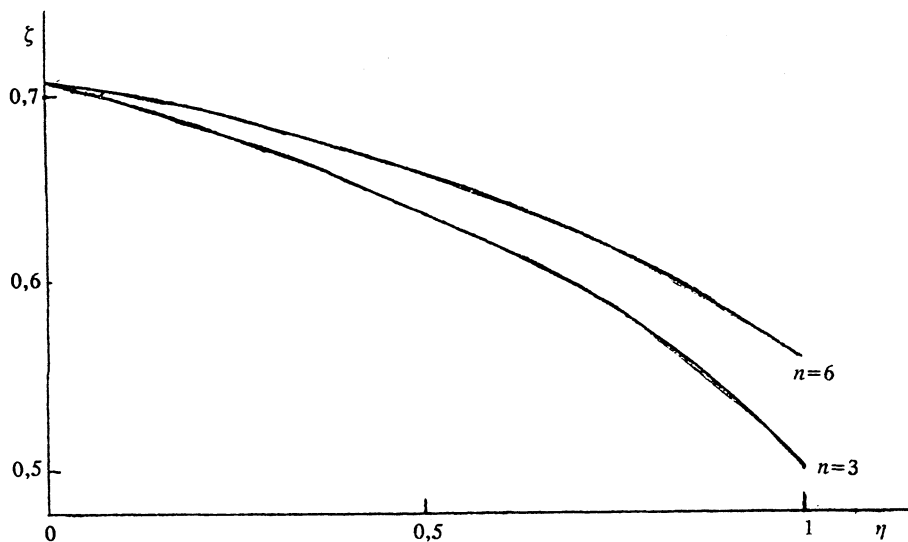


FIG. 3. Position of the point of the quasi-isotropy of the collisional relaxation of the polarization moments of the laser-excited atoms A in the plane of the dimensionless parameters J and η [see (7)] for an A-B interaction law of the $1/R^n$ type, where $n=3$ or 6.

velocity distribution increases with distance from this boundary line and also with increasing distance from the abscissa. It reaches its maximum values at $\eta=1$, i.e., in the limit $M_B/M_{jA} \rightarrow \infty$. This result emphasizes once more the benefit of using a background gas B as heavy as possible for the laser imposition of an anisotropy in the distribution of the relative velocities of colliding atoms A and B.

The vanishing of the dynamic quadrupole moment of velocity distribution (30) is a necessary condition for a quasi-isotropic relaxation. This condition is not the same as the approximate condition for a quasi-isotropy based on the requirement that the mean square velocities of the colliding particles along the three coordinate axes be identical [see (8)]. On the other hand, this approximate condition yields the value $\zeta=0.71$ for the point of quasi-isotropy for all values of the parameter η . The solution of Eq. (30) yields η -dependent values of the parameter ζ which lead to quasi-isotropic relaxation. Figure 3 shows the results of a solution of this equation for two particle interaction laws (13), with exponents $n=6$ and 3. We see that the quasi-isotropy point lies at $\zeta=0.71$ only in the limit of a vanishingly small mass of the B particles, i.e., only in the case $\eta=0$. For nonzero masses of the particles of the impurity gas B, with $\eta \neq 0$, the quasi-isotropy point $\zeta(\eta)$ is significantly smaller than 0.71, and its position varies with the exponent n in the particle interaction law. This result means that the points of quasi-isotropic collisional relaxation shift toward the center of the Doppler profile with increasing mass ratio M_B/M_A ; this shift is greater for the case of collisions of excited A atoms with B ions ($n=3$) than for collisions of these atoms with neutral B particles ($n=6$).

At the quasi-isotropy point, only the dynamic quadrupole moment S_2 of the velocity distribution vanishes; higher-order dynamic quadrupole moments may be nonzero. At this point there is accordingly partial conservation of the anisotropic nature of the collisional relaxation, due to the mutual conversion of the higher polarization moments in which dynamic multipole moments S_4, S_6, S_8 ,

etc., of the velocity distribution are involved.

To summarize this and the preceding sections of the paper, we could say that the material presented here forms a closed theory for the anisotropic collisional relaxation of the polarization moments of an ensemble of atoms excited in a gaseous medium by monochromatic laser light. (This assertion is made at the level of accuracy of this discussion, which is determined by the impact-parameter method, by the rectilinear-trajectory approximation, and by the power-law interaction of the colliding particles.) All the diverse collisional relaxation processes are described by Eqs. (3) under these conditions. The rate constants $\langle v\sigma_q^{KK1} \rangle$ which appear in these equations are calculated from (21) and are determined by the characteristics of the extremely anisotropic collisional relaxation of the polarization moments in the oppositely directed monoenergetic particle beams—the coefficients a_q^{KK1} [see (14)], which were calculated and tabulated in Ref. 51. They are also determined by the dynamic multipole moments of the velocity distribution [see (23)]. The latter depend on the dimensionless parameters ζ and η , given by (7). By varying the detuning of the laser frequency from the center of the Doppler profile of the spectral line, one can smoothly vary the anisotropic nature of the relaxation (through the parameter ζ). In turn, the anisotropy of the relaxation becomes more pronounced with increasing value of the parameter η , i.e., of the mass ratio M_B/M_A of the atoms of the background gas B and the substance under study, A.

In the following sections of this paper we look at some specific applications of this theory to various manifestations of an anisotropic collisional relaxation of atomic polarization moments during monochromatic laser excitation.

6. COLLISIONAL CONVERSION OF THE ALIGNMENT OF ATOMIC ANGULAR MOMENTA INTO AN ORIENTATION OF THESE MOMENTA DURING LASER EXCITATION

One of the most characteristic features of anisotropic collisional relaxation of atomic polarization moments is the

appearance of an orientation from alignment, accompanied by the appearance of circular polarization of the light.^{9,10} This effect is based on a joint collisional relaxation of the orientation components $\rho_{\pm 1}^1$, transverse with respect to the anisotropy axis, and the alignment components $\rho_{\pm 1}^2$, which make at an angle of 45° with this axis. The collisional creation of an orientation thus requires that these tilted components of the alignment be set up beforehand. Since the light waves are transverse, only the longitudinal component ρ_0^2 and the transverse components $\rho_{\pm 2}^2$ of the alignment (with respect to the laser beam) arise during excitation of the atoms. To create the tilted components of the alignment, one should apply a magnetic field directed across the laser beam (along the x axis); this field will rotate the original alignment and give rise to the components $\rho_{\pm 1}^2$.

Under these conditions the time evolution of the polarization moments of the excited atoms is described by the equations

$$\dot{\rho}_q^K = -\Gamma_0 \rho_q^K - n_B \sum_{\kappa_1} \langle v \sigma_q^{\kappa \kappa_1} \rangle \rho_q^{\kappa_1} + \omega_L \sum_{q_1} H_{qq_1}^K \rho_{q_1}^K + N_q^K, \quad (31)$$

where Γ_0 is the radiative-decay constant, N_q^K is the intensity of the optical nucleation of the polarization moment ρ_q^K , ω_L is the Larmor precession frequency of the angular momentum \mathbf{J} in a magnetic field parallel to the x axis, and the elements of the matrix H are given by

$$H_{qq_1} = -\frac{i}{2} \left[\sqrt{(\kappa - q)(\kappa + q + 1)} \delta_{q_1, q+1} + \sqrt{(\kappa + q)(\kappa - q + 1)} \delta_{q_1, q-1} \right]. \quad (32)$$

We solved Eqs. (31) in the steady state for various values of the angular momentum ($J=1, 3/2$, and 2) of the excited state of atoms A for various detunings of the laser frequency, represented by the parameter ξ in (7), and for various colliding-particle interaction laws (13), with $n=6$ or 3 .

The efficiency for orientation of angular momenta of the excited atoms to result from their alignment is characterized by the ratio

$$P = \max(I_{\sigma^+} - I_{\sigma^-}) / (I_y - I_z)_0. \quad (33)$$

The numerator contains that maximum difference between the intensities of the light of left-hand and right-hand circular polarizations in the case of observation along the x axis which can be achieved by varying the magnetic field strength. The numerator contains the difference between the intensities of the light of linear polarizations measured in a zero magnetic field. The presence of this maximum corresponds to the particular magnetic field which leads to the maximum values of the alignment components $\rho_{\pm 1}^2$ tilted from the z axis (for given rates of radiative decay and collisional relaxation).

The results of our calculations are shown in Fig. 4. This figure shows P in (33) for collisions of excited atoms in states with angular momenta $J=1, 3/2$, and 2 with neutral atoms (the solids lines) and with ions (dashed lines),

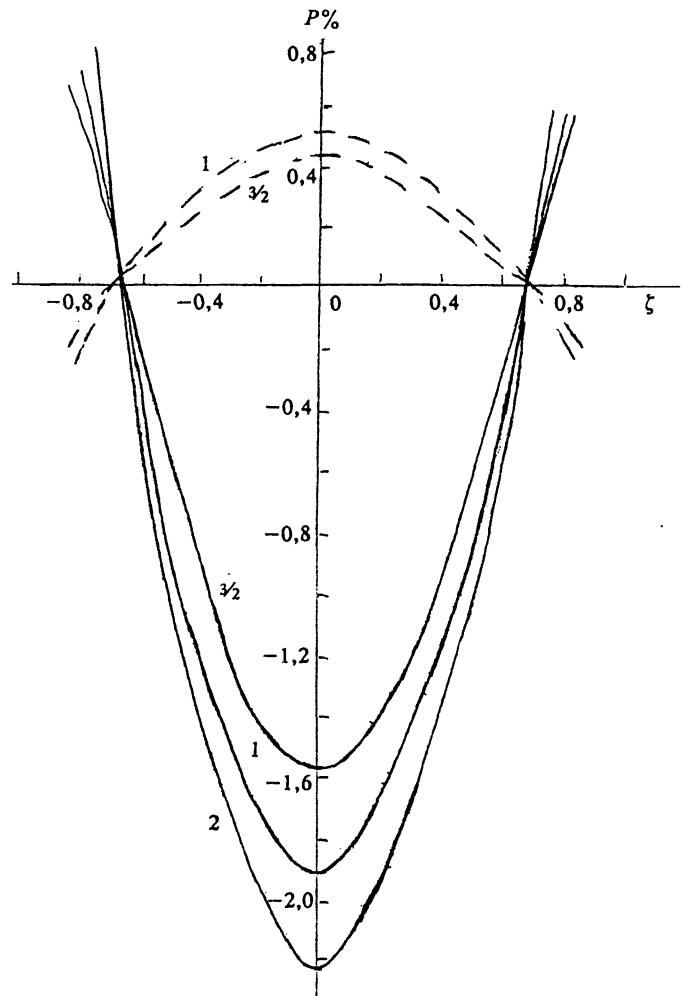


FIG. 4. Calculated ratio of the signals of the circular and linear polarizations of the light versus the laser-frequency detuning parameter J for the case in which excited A atoms in a state with angular momentum $J=1, 3/2$, or 2 undergo anisotropic collisions with neutral (solid curves) or charged (dashed curves) particles of the background-gas atoms B. The calculations were carried out for identical masses of the A and B atoms.

for various detunings of the laser frequency. These calculations correspond to the case of identical masses of the A and B particles ($\eta=1/2$) and to light which is emitted upon the transition of an atom from the given excited state J to a state with an angular momentum $J_0=J-1$, under conditions such that the "dimensionless pressure" of the background gas,

$$u = \frac{n_B}{\Gamma_0} \left[\frac{2kTM_A M_B}{(M_A + M_B)} \right]^{(n-3)/2(n-1)} \left(\frac{\Delta C}{\hbar} \right)^{2/(n-1)}, \quad (34)$$

is unity. For transitions to states with other angular momenta, the corresponding efficiencies for initiation of circular polarization of the light can be found from the proportions

$$P(J \rightarrow J+1) : P(J \rightarrow J) : P(J \rightarrow J-1) = \begin{cases} -5 : -1 : 1, & J=1, \\ -6 : -1 : 1, & J=3/2, \\ -7 : -3 : 3, & J=2. \end{cases} \quad (35)$$

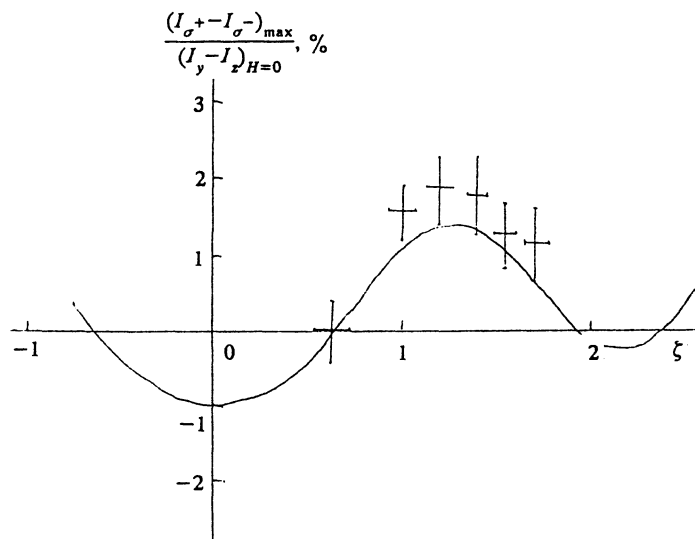


FIG. 5. Calculated ratio of the signals of the circular and linear polarizations of the light for an anisotropic collisional creation of orientation from alignment for neon atoms in the ${}^2p_43p[3/2]_2$ state, $J=2$ in the natural isotope mixture, 91% ${}^{20}\text{Ne}$ and 9% ${}^{22}\text{Ne}$. The parameter J determines the detuning of the laser frequency from the center of the Doppler absorption line of the isotope ${}^{20}\text{Ne}$. The crosses are experimental data.¹⁵

We see from this figure that the circular-polarization signals (and the corresponding orientations of the atomic angular momenta) differ in sign for the cases in which the excited A atoms collide with neutral particles and with ions. This result is evidence that the collisional nucleation of orientation from alignment is sensitive to the particle interaction law. The orientation signals have (in absolute value) local maxima for zero detuning of the laser frequency ($\zeta=0$). These local maxima reach 2% in the case of collisions with neutral B particles and 0.5% for collisions with ions. As the detuning of the laser frequency is increased from zero to the quasi-isotropy points (near $\zeta=0.7$), the efficiency of the nucleation of orientation falls off to zero. As the parameter ζ is increased further (i.e., in the wings of the Doppler profile), this efficiency changes sign and begins to increase rapidly in absolute value.

The efficiency of the collisional nucleation of orientation also depends on the angular momentum of the excited atomic state. For collisions of excited atoms with neutral particles, this efficiency is at a maximum in the case $J=2$; it decreases as we go to $J=1$ and then to $J=3/2$. For collisions with B ions, it is at a maximum at $J=1$, it is slightly smaller at $J=3/2$, and it is essentially zero at $J=2$, in which case the matrix element corresponding to the transition from alignment to orientation is two orders of magnitude smaller⁵¹ than for $J=1$ or $3/2$.

The case $M_A=M_B$, which we are discussing here, corresponds to experimental conditions under which orientation has been observed¹⁵ to arise from alignment for neon atoms in the $2p_4(3p[3/2]_2)$, $J=2$ state excited by a single-mode laser with a tunable frequency. These atoms were subjected to anisotropic collisions with unexcited neon atoms in a magnetic field perpendicular to the laser beam. In accordance with the experimental conditions, our calculations were carried out for the natural mixture of neon isotopes (91% ${}^{20}\text{Ne}$ and 9% ${}^{22}\text{Ne}$), for a temperature of 400 K and a pressure of 1.3 torr. The overlap of the Doppler profiles of the isotopes ${}^{20}\text{Ne}$ and ${}^{22}\text{Ne}$, which are shifted 1.72 GHz from each other, was taken into account. For each given laser frequency, Eqs. (31) were solved for both

isotopes; the laser-frequency dependence of the efficiency of their optical excitation and of the relaxation rate constants was taken into account. The overall orientation efficiency, (33), was calculated with allowance for the contributions of both isotopes (taken with weights of 0.91 and 0.09) to the circular- and linear-polarization signals. The results of these calculations are shown in Fig. 5, where the laser-frequency detuning parameter ζ corresponds to a shift of the laser frequency with respect to the center of the Doppler profile of the isotope ${}^{20}\text{Ne}$. The crosses show experimental data from Ref. 15, which were obtained at the optimum value of the static magnetic field (approximately 5 G).

The calculated orientation signal P crosses zero and changes sign at four points: $\zeta_1=-0.66$, $\zeta_2=0.63$, $\zeta_3=2.0$, and $\zeta_4=2.3$. The points ζ_1 and ζ_2 are close to the points of a quasi-isotropy of the relaxation for the isotope ${}^{20}\text{Ne}$ by itself ($\zeta=\pm 0.66$). The other two zeros of the orientation signal (ζ_3 and ζ_4) lie a significant distance away from the quasi-isotropy points for the isotope ${}^{22}\text{Ne}$ by itself. These points are symmetric with respect to the center of the Doppler profile of its spectral line ($\zeta=1.78$) and lie at the points $\zeta=1.11$ and $\zeta=2.45$. The reason for the shift of the zeros away from the quasi-isotropy points for the pure isotopes ${}^{20}\text{Ne}$ and ${}^{22}\text{Ne}$ on the plot in Fig. 5 is a superposition of the Doppler profiles of the spectral lines of the two isotopes: It is negligible for the point ζ_1 , small for ζ_2 , and quite noticeable for ζ_4 and ζ_3 .

The oscillatory nature of the signal representing the orientation induced by anisotropic collisions as a function of the frequency of the monochromatic exciting light can thus be utilized to experimentally determine the positions of the points of a quasi-isotropic relaxation. The existence of more than two zeros for this function at a zero nuclear spin indicates that the gas under study contains two or more isotopes. For atoms with a nonzero nuclear spin the corresponding dependence is more complicated, having a number of zeros equal to twice the number of hyperfine-structure components even in the case of pure isotopes.

7. COLLISIONAL INITIATION OF ALIGNMENT DURING MONOCHROMATIC LASER EXCITATION

We assume that a monochromatic laser beam excites the atoms under study (of type A) into a state with a total electron-nuclear angular momentum $F=1/2$. There are no polarization moments of higher than the first rank in this state, so there is no alignment (second-rank polarization moment). The excited atoms, whose component of the velocity v_0 along the laser beam [see (4)] is selected by the monochromatic light, undergo anisotropic collisions with atoms of the surrounding gaseous medium. These collisions lead in particular to transitions of these atoms to states with $F \neq 1/2$. In these states, along with the populations ρ_0^0 , the anisotropic collisions cause longitudinal components of four higher-rank polarization moments, including an alignment component ρ_0^0 of the angular momentum F along the laser beam. As a result, the sensitized fluorescence emitted by atoms from levels filled by anisotropic collisions will be partially linearly polarized along the laser beam.

This mechanism for the collisional initiation of alignment and the appearance of a linear polarization of light in the course of anisotropic, collisional, intermultiplet mixing was studied experimentally in Ref. 23 in the case of a selective laser excitation of hyperfine levels of the $(3p)^2P_{1/2}$ state, with detection of the linear polarization of the sensitized fluorescence emitted from the $(3p)^2P_{3/2}$ state of sodium atoms in a xenon atmosphere.

A theory of this process must incorporate the effect of collisions on both the electron angular momentum \mathbf{J} and the resultant electronic-nuclear angular momentum of the atom, $\mathbf{F}=\mathbf{J}+\mathbf{I}$, where \mathbf{I} is the nuclear spin. This can be done in a model of the disruption of both the fine and hyperfine coupling at the time of the collision: Such a model assumes that the splitting of levels with different projections of the electron orbital angular momentum \mathbf{L} of the A atom onto the A-B direction is significantly larger than not only the hyperfine splitting but also the fine splitting of levels. During the collision we thus have a sort of analog of the Paschen-Back effect: The electron orbital angular momentum \mathbf{J} of the atom reacts to the collision and undergoes a change in projection, while neither the nuclear spin \mathbf{I} nor the electron spin \mathbf{S} "is fast enough" to react to the collision. Each retains the same projection. As a result, the collisional relaxation of the polarization moments constructed for the electron orbital angular momentum \mathbf{L} is determined by the corresponding rate constants in Eq. (3). The relaxation of the electronic-nuclear polarization moments $\rho_Q^K(F)$ corresponding to the resultant atomic angular momentum \mathbf{F} can then be calculated with allowance for the relaxation law for the angular momentum \mathbf{L} and the generalized scheme for combining angular momenta.¹⁸

The resultant electronic-nuclear polarization moments $\rho_Q^K(F)$ of the hyperfine levels of the atom are related to the

density matrix elements of these levels by the transformation

$$\rho_Q^K(F) = \sum_{MM_1} (-1)^{F-M_1} \begin{bmatrix} F & F & K \\ M & -M_1 & Q \end{bmatrix} \sigma_{FM,FM_1}, \quad (36)$$

where M and M_1 are the magnetic quantum numbers for the angular momentum F . Using a different representation of the electronic-nuclear density matrix, $\sigma_{m\mu,m_1\mu_1}$, which corresponds to the values found for the magnetic quantum numbers of the electron angular momentum (m and m_1) and the nuclear spin (μ and μ_1), we can construct electron polarization moments of the atom for fixed projections of the nuclear spin μ and μ_1 onto the z axis:

$$\rho_{q,\mu\mu_1}^\kappa = \sum_{mm_1} (-1)^{J-m_1} \begin{bmatrix} J & J & \kappa \\ m & -m_1 & q \end{bmatrix} \sigma_{m\mu,m_1\mu_1}. \quad (37)$$

Substituting (37) into (36), we find the following expression for the electron-nuclear polarization moments corresponding to definite hyperfine levels:

$$\begin{aligned} \rho_Q^K(F) = & \sum_{MM_1} \sum_{mm_1\mu\mu_1} \sum_{\kappa q} (-1)^{F-M_1} \\ & \times \begin{bmatrix} F & F & K \\ M & -M_1 & Q \end{bmatrix} \begin{bmatrix} J & I & F \\ m & \mu & M \end{bmatrix} \\ & \times \begin{bmatrix} J & I & F \\ m_1 & \mu_1 & M_1 \end{bmatrix} \begin{bmatrix} J & J & \kappa \\ m & -m_1 & q \end{bmatrix} \rho_{q,\mu\mu_1}^\kappa. \end{aligned} \quad (38)$$

Under the conditions for the applicability for the model of the disruption of the hyperfine coupling, the nuclear-spin part of the density matrix does not change in the course of collisions. The effect of collisions on the electronic-nuclear polarization moments is thus determined by their effect on the quantities $\rho_{q,\mu\mu_1}^\kappa$ on the right side of (38). These quantities relax under the influence of collisions in terms of their indices κ and q in precisely the same way as the purely electron polarization moments ρ_q^κ do, i.e. in accordance with the equations for anisotropic relaxation in (3). The indices μ and μ_1 remain the same; this situation corresponds to a conservation of the orientation of the nuclear spin during the collision (the "principle of nuclear-spin inertia"⁵³). We can thus use Eqs. (3) and the generalized technique for combining angular momenta to derive from (38) equations describing the time evolution of the electron-nuclear polarization moments of the hyperfine levels under laser-excitation conditions:

$$\begin{aligned} \dot{\rho}_Q^K(F) = & -\Gamma_0 \rho_Q^K(F) + N_Q^K(F) - n_B(2F+1) \sqrt{2K+1} \sum_{K_1 F_1} (2F+1) \sqrt{2K_1+1} \sum_{\kappa \kappa_1 p} (-1)^{p+q+Q} \sqrt{(2\kappa+1)(2\kappa_1+1)} \\ & \times \left\langle \begin{array}{ccc} J & J, \kappa & \kappa_1, J \\ I & p & I \\ F & F_1, K & K_1, F \\ & & F_1 \end{array} \right\rangle \begin{bmatrix} \kappa_1 & \kappa & p \\ q & -q & Q \end{bmatrix} \begin{bmatrix} K_1 & K & p \\ Q & -Q & 0 \end{bmatrix} \langle v \sigma_q^{\kappa \kappa_1}(J) \rangle \rho_Q^{K_1}(F_1). \end{aligned} \quad (39)$$

The first two terms on the right side describe the radiative decay and optical excitation of the electron-nuclear polarization moment $\rho_Q^K(F)$; the third describes the collisional relaxation of this moment. The angle brackets denote the $15j$ symbol as defined in Ref. 12.

During laser excitation of ^{23}Na sodium atoms, with a nuclear spin $I=3/2$, optical transitions between hyperfine states occur: $(3s) \ ^2S_{1/2}(F_0=1 \text{ or } 2) \rightarrow (3p) \ ^2P_{1/2}(F=1 \text{ or } 2)$. Correspondingly, there are four overlapping Doppler profiles of the hyperfine absorption line. During the absorption of a photon of monochromatic laser light with a given frequency ν , four groups of excited atoms thus arise in the $^2P_{1/2}$ state with different values of the projection of the velocity v_0 onto the axis of the laser beam [these projections are determined by the detuning $(\Delta\nu)$ of the frequency from the center of the corresponding Doppler profile; see (4)]. It thus becomes necessary to solve Eqs. (39) separately for each of the four groups of atoms, corresponding to the four light absorption channels.

Equations (39) constitute a system of relaxation equations describing the collisional mixing of the hyperfine-structure multiplets and the nucleation of an alignment, in which we are interested. They relate the longitudinal electron-nuclear polarization moments of even ranks ($K=0, 2, 4$, and 6) in (38) to the $Q=0$ components of the hyperfine structure of the $^2P_{1/2}$ and $^2P_{3/2}$ excited electronic states, of which there are a total of 27. This system of 27 equations was solved for each of the four groups of atoms for various deviations of the laser frequency from the centers of the hyperfine components of the spectral line, for various background inert gases, and for various pressures. The cycle of optical pumping in the system of hyperfine levels of the $(3s) \ ^2S_{1/2}$ and $(3p) \ ^2P_{1/2}$ states participating in the absorption of light was taken into account. The resultant population and alignment of the hyperfine levels of the $^2P_{3/2}$ electronic state were calculated as the sums of the contributions of all four groups of atoms (weighted in accordance with the light absorption intensities in the four channels for excitation of the sodium atoms).

Figure 6 shows a calculated alignment signal, i.e., the intensity difference $(I_z - I_x)$ of the sensitized fluorescence polarized along the laser beam and perpendicular to it, emitted by sodium atoms from the $(3p) \ ^2P_{3/2}$ state, filled by collisions, in a xenon atmosphere (at a pressure of 1 torr and a temperature of 383 K). The solid line is the resultant signal, while the dashed lines 1-4 are the contributions of the groups of atoms excited in transitions involving the absorption of a laser photon between the following hyperfine levels of the $(3s) \ ^2S_{1/2}$ and $(3p) \ ^2P_{1/2}$ states, respec-

tively: $F_0=1 \rightarrow F=1$, $F_0=1 \rightarrow F=2$, $F_0=2 \rightarrow F=1$ and $F_0=2 \rightarrow F=2$. The width of the calculated alignment signal is 0.026 cm^{-1} , and its peak corresponds to a 2% linear polarization. These results agree well with the experimental data of Ref. 23 (0.028 cm^{-1} and 1.6%). We thus have evidence that not only the general equations of the theory of anisotropic collisional relaxation but also the model used here for the disruption of the hyperfine structure and the narrow fine structure can be applied to a detailed description of the process of collisional nucleation of alignment during laser excitation of atoms.

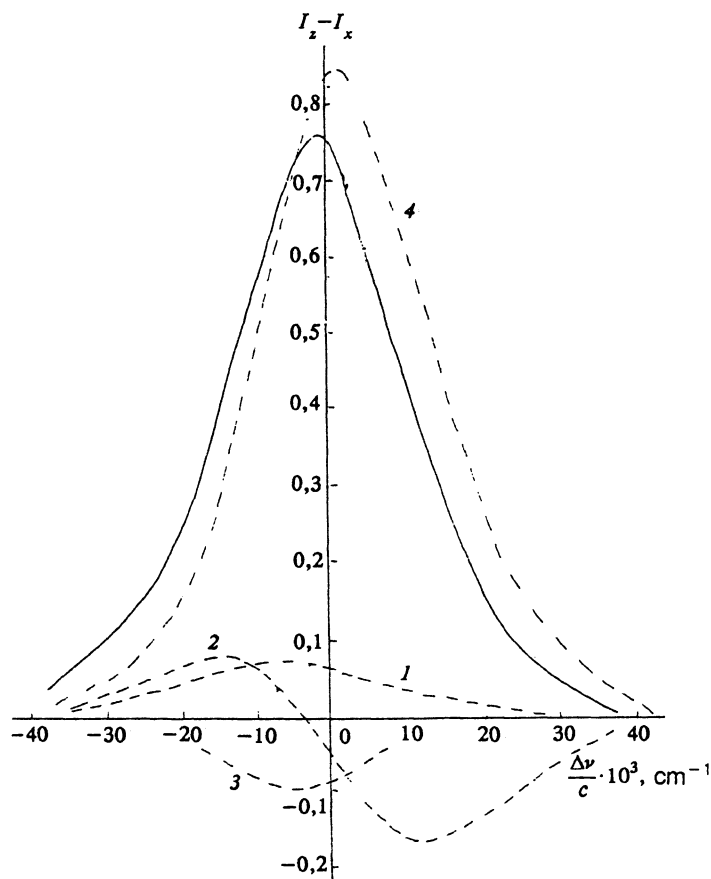


FIG. 6. Signal representing the linear polarization of the sensitized fluorescence light emitted by sodium atoms from the $3p \ ^2P_{3/2}$ state, populated by anisotropic collisions with atoms of the background gas (xenon) versus the detuning of the laser frequency, $\Delta\nu$ (solid curve). The dashed curves describe the contributions of the four groups of sodium atoms excited in transitions between the following pairs of hyperfine levels of the $3s \ ^2S_{1/2}$ ground state: 1— $F_0=1 \rightarrow F=1$; 2— $F_0=1 \rightarrow F=2$; 3— $F_0=2 \rightarrow F=1$; 4— $F_0=2 \rightarrow F=2$.

8. RATES OF COLLISION-INDUCED TRANSITIONS BETWEEN ATOMIC LEVELS AS FUNCTIONS OF THE FREQUENCY OF THE MONOCHROMATIC LASER LIGHT

The collisional mixing of the longitudinal components of the even polarization moments of various ranks under anisotropic conditions leads to collisional nucleation of an alignment ρ_0^2 from the populations ρ_0^0 of the atomic states. There is, on the other hand, the further possibility of the inverse process: essentially an effect of an existing alignment ρ_0^2 on the collisional transfer of populations ρ_0^0 between atomic levels as a result of anisotropic collisions.³⁶⁻⁴⁵ There is thus the possibility of controlling the rates of the collision-induced transitions between atomic states by varying the frequency of the exciting laser light. This approach makes it possible to change the sign and magnitude of the dynamic quadrupole moment of the distribution function.

According to the calculations of Ref. 37, the rate constant for the collisional transfer of populations between the $J=3/2$ and $J=1/2$ levels of the narrow 2P fine-structure doublet in the course of extremely anisotropic collisions in oppositely directed particle beams associated with a change in the optical alignment of the $^2P_{3/2}$ level increases by a factor of 4 in collisions with charged particles, and by a factor of 6 in collisions with neutral particles. It reaches a maximum in the case of excitation of the $^2P_{3/2}$ state by light which is linearly polarized perpendicular to the common axis of the particle beams; it reaches a minimum when the light is polarized along this axis. In the first case the light induces a positive alignment along the anisotropy axis (the z axis) in the $^2P_{3/2}$ level, and the efficiency of the $J=3/2 \rightarrow J=1/2$ collisional transitions increases. In the second case, the light induces a negative alignment, and the efficiency of the collisional transitions between levels is suppressed. Corresponding results were later obtained for the collisional transfer of population between the 3P_1 and 3P_2 states of the excited atoms of inert gases.⁴⁴ The efficiency of this transfer in the case of extremely anisotropic collisions in oppositely directed beams changes by a factor up to ten, depending on the polarization of the exciting light, and for collisions of excited sodium atoms with helium atoms, in which case the calculations described a change by a factor up to 3 in the rate of collisional transfer of populations.⁴⁰⁻⁴²

This theoretically predicted dependence of the rates of collisional transfer of populations between atomic states on their alignment has yet to be studied experimentally. In this paper we present a theory for this effect, for collisional transition between hyperfine levels during monochromatic laser excitation, for the experimental conditions of Ref. 54. In that study, an experimental method was developed for investigating the collisional transfer of populations (in the absence of alignment) between the $F=3/2$ and $F=1/2$ hyperfine levels of the $(5s5p) ^3P_1$ excited state of the ^{113}Cd cadmium atom. The resonance transition of a cadmium atom from the ground state to this excited state has a wavelength of 326.1 nm; the distance between the hyperfine levels is 0.216 cm^{-1} , and the half-width of the Doppler line is 0.022 cm^{-1} (at 455 K).

Since there is essentially no overlap of the Doppler profiles of the various components of the hyperfine structure in this case, it is possible to optically excite each hyperfine level separately. At the same time, the hyperfine structure is negligibly small in comparison with the fine splitting of the $(5s5p) ^3P$ level (1713 cm^{-1}) and also in comparison with the average thermal energy of the colliding particles (320 cm^{-1}). Consequently, the model for the disruption of the hyperfine structure during a collision which was described in the preceding section of this paper is well justified. At the same time, the fact that the thermal energy is small in comparison with the fine level splitting means that the angular momentum \mathbf{J} of the electron cloud is conserved in magnitude, while undergoing a change in orientation during the collision in accordance with the differential equations of the impact-parameter method. The equations for the relaxation of the populations $n_{1/2}$ and $n_{3/2}$ of the $F=1/2$ and $F=3/2$ hyperfine levels and for the alignment $a_{3/2}$ of the $F=3/2$ hyperfine level become

$$\begin{aligned} \dot{n}_{1/2} &= -(\Gamma_0 + 2W_1)n_{1/2} + W_1n_{3/2} + W_2a_{3/2}, \\ \dot{n}_{3/2} &= 2W_1n_{1/2} - (\Gamma_0 + W_1)n_{3/2} - W_2a_{3/2} + N_{3/2}, \\ \dot{a}_{3/2} &= 2W_2n_{1/2} - W_2n_{3/2} - (\Gamma_0 + W_3)a_{3/2} + A_{3/2}. \end{aligned} \quad (40)$$

The alignment in these equations is related to the population of the $F=3/2$ level by

$$a_{3/2} = \frac{3\langle F_z^2 \rangle - F(F+1)}{F(2F-1)} n_{3/2}, \quad (41)$$

where the angle brackets mean an average over the ensemble of excited atoms. Here $N_{3/2}$ and $A_{3/2}$ are the intensities of the optical filling of the $F=3/2$ hyperfine level and the induction of an alignment involving this level, Γ_0 is the radiative-decay constant (which is $4.18 \cdot 10^5 \text{ s}^{-1}$ for this excited state of the cadmium atom). The quantities W_1 , W_2 , and W_3 are respectively the rate of the collision-induced transfer of populations between hyperfine levels, the rate of collisional conversion of the alignment of the $F=3/2$ level into the populations of the $F=1/2$ and $F=3/2$ levels, and the rate of collisional destruction of the alignment involving the $F=3/2$ level. It can be seen from Eqs. (40) that the contributions of the alignment $a_{3/2}$ to the changes in the populations of the $F=1/2$ and $F=3/2$ levels cancel out: The alignment affects the rate of the redistribution of population between the levels of the hyperfine doublet, but not its total population $n_{1/2} + n_{3/2}$.

The quantities W_1 , W_2 , and W_3 are expressed in terms of the rate constants of the anisotropic collisional relaxation of the electron polarization moments ρ_q^k of the $J=1$ state and the dynamic multipole moments of the velocity distribution in (22). Here relations (38) between the electron and electron-nuclear polarization moments are taken into account.

We constructed and solved system of equations (40) for both pulsed and *cw* excitation of the atoms by monochromatic laser light, for various detunings of the laser frequency from the center of the Doppler profile of the hyperfine line corresponding to excitation of the $F=3/2$

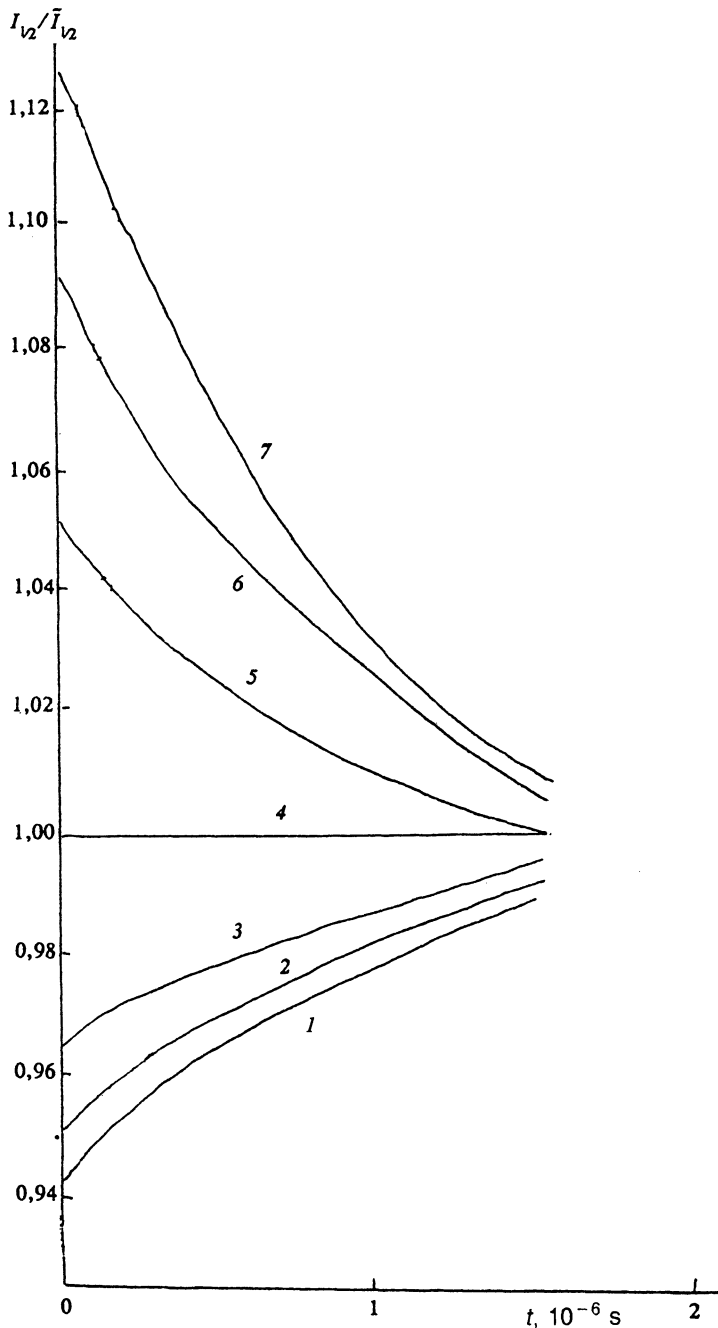


FIG. 7. Effect of the degree of alignment of the $F=3/2$ hyperfine level of the $5s5p\ ^3P_1$ electronic state of the ^{113}Cd atoms and the detuning of the laser frequency on the collisional transport of population from this level to the hyperfine level $F=1/2$. The quantity $I_{1/2}/\bar{I}_{1/2}$ is the ratio of the time-dependent intensities of the sensitized-fluorescence signals emitted from the $F=1/2$ level in the presence and absence of an optical alignment of the $F=3/2$ level, respectively. The curves were found for the following values of the detuning of the laser frequency: 1— $\Delta\nu=0$; 2—0.005; 3—0.010; 4—0.0174; 5—0.025; 6—0.035; 7—0.045 cm^{-1} . The calculations were carried out for 455 K and for a background-gas (xenon) pressure of 0.08 torr.

hyperfine level of the $(5s5p)\ ^3P_1$ state of the ^{113}Cd atom, for various degrees of alignment $a_{3/2}$ of the $F=3/2$ level. The degree of alignment was found from

$$a = a_{3/2}/n_{3/2}. \quad (42)$$

Using (41), we see that the values of this quantity which are theoretically possible for the $F=3/2$ state are from -1 to $+1$.

The curves in Fig. 7 reveal the effect of the alignment of the $F=3/2$ level on the transfer of population from this laser-excited level to the $F=1/2$ level for various detunings of the laser frequency. The abscissa here represents time, measured from the light pulse; the ordinate is the calculated intensity ratio of the signals of the sensitized fluorescence emitted from the $F=1/2$ level in the case in which

there is an alignment at the $F=3/2$ level (induced by the laser pulse) and for the case in which this alignment is suppressed by a magnetic field (this method for suppressing the alignment was used in Ref. 54). Comparison of the curves in Fig. 7 shows that in the region of small detunings, from the center of the Doppler profile to the quasi-isotropy point ($0 \leq |\Delta\nu| \leq \Delta\nu_0 = 0.0174\ \text{cm}^{-1}$), the alignment slows the collisional transfer of population, while at large detunings ($|\Delta\nu| > \Delta\nu_0$) it accelerates this process.

In this case the alignment induced by the laser pulse is positive: $A_{3/2} = N_{3/2}/2 > 0$. The collisional transfer of population is thus accelerated when the alignment of the initial level has the same sign as the dynamic quadrupole moment of the relative-velocity distribution; it slows down in the

TABLE II. Rate constants of the collisional relaxation of the populations and alignment of the hyperfine levels of the $5s5p\ ^3P_1$ electronic state of the ^{113}Cd atoms versus the detuning of the laser frequency from the center of the Doppler profile.

Frequency detuning, cm^{-1}	0	0,005	0,010	0,015	0,025	0,035	0,045
$\langle v\sigma_p \rangle$	7,38	7,43	7,55	7,74	8,30	9,03	9,83
$\langle v\sigma_a \rangle$	-0,77	-0,70	-0,50	-0,18	0,70	1,73	2,81
$\langle v\sigma_d \rangle$	10,2	10,3	10,6	11,0	12,2	13,7	15,3

opposite case. At the quasi-isotropy point ($\Delta\nu = \Delta\nu_0$) the dynamic quadrupole moment of the distribution function disappears, and the alignment has no effect on the collisional transfer of population.

The effect of the alignment on the population transfer is most obvious shortly after the pulsed excitation, when the collisional relaxation is just beginning. At the point $t=0$ the rate of population transfer in the case with an alignment is 95% (for excitation at the center of the Doppler profile) and 114% (for excitation in the wing of the profile, $\Delta\nu = 0.045\ \text{cm}^{-1}$) of its velocity in the absence of alignment.

All the collisional relaxation processes described here are governed by the coefficients W_1 , W_2 , and W_3 in Eqs. (40). The latter are related to the rate constants for the collisional transfer of population, $\langle v\sigma_p \rangle$, the collisional mutual conversion of alignment and populations, $\langle v\sigma_a \rangle$, and the collisional destruction of alignment (depolarization), $\langle v\sigma_d \rangle$, by

$$W_1 = n_B \langle v\sigma_p \rangle, \quad W_2 = n_B \langle v\sigma_a \rangle, \quad W_3 = n_B \langle v\sigma_d \rangle, \quad (43)$$

where n_B is the density of background gas B. The rate constants which we calculated for the ^{113}Cd cadmium atoms in the $(5s5p)\ ^3P_1$ state, $F=3/2$ and $1/2$, in a xenon atmosphere at 455 K, are shown in the three rows in Table II for various detunings of the laser frequency from the center of the Doppler profile of the hyperfine components of the $(5s^2)\ ^1S_0(F=1/2) \rightarrow (5s5p)\ ^3P_1(F=3/2)$ absorption line. It can be seen from Table II that as we go from excitation at the center of the Doppler profile to excitation in its wing (to a detuning twice the half-width of the profile) the rate constant for the transfer of population increases by a third, and that for depolarization by a factor of 1.5. The rate constant for the mutual conversion of alignment and population, which is specific to anisotropic collisional relaxation, changes sign (at the quasi-isotropy

point) as the detuning is increased; its absolute value in the wing of the profile is 3.7 times that at the center.

The comparatively weak effect of the alignment on the rate of population transfer between hyperfine levels during laser excitation (weak in comparison with the case of an extremely anisotropic relaxation of the purely electronic angular momentum $J=1$, discussed in Ref. 37) stems from three factors: First, the anisotropic nature of the relaxation is smoothed out when we switch from fine-structure levels to hyperfine levels as a result of the "principle of nuclear-spin inertia." The nuclear spin does not react immediately to collisions. Second, during laser excitation the velocity distribution is only partially anisotropic. Third, instead of the theoretically maximum possible positive or negative degree of alignment [see (42)] of the $F=3/2$ level ($a_{3/2} = \pm 1$), the degree of alignment of this level induced by the laser light is only half the maximum possible ($a_{3/2} = 1/2$). We thus immediately see ways to raise the effect of the detuning of the laser frequency on the rate of population transfer between atomic levels: Raise the anisotropy of the velocity distribution through the use of excitation further out on the wing of the Doppler profile, use a background gas as heavy as possible, raise the degree of alignment of the atomic angular momenta, and, finally, switch from a hyperfine multiplet to a narrow fine-structure multiplet. For such multiplets the degree of alignment can be raised by applying a weak magnetic field parallel to the laser beam. Such a field does not suppress the alignment which arises during absorption of the light, but it does make it possible to separate the Zeeman levels with the maximum ($|m_J| = J$) and minimum ($|m_J| = 0$ or $1/2$) absolute values of the projection of the angular momentum onto the direction of the laser beam. Selective laser excitation of these Zeeman levels makes it possible to easily reach the maximum negative degree of alignment

(with $m_J=0$ or $1/2$) and maximum positive degree of alignment (with $|m_J|=J$) of the electron angular momenta of the excited atoms along the laser beam.

This method makes it completely feasible to adjust the rate constants for the collisional transfer of populations between fine-structure levels by a factor up to 2 or 3 by varying the laser frequency.

9. LIGHT POLARIZATION BEATS DURING LASER EXCITATION

Light polarization beats⁴⁶⁻⁴⁹ are a manifestation of a coupling of polarization moments of different ranks κ in transient processes during an anisotropic collisional relaxation. The simple one-exponential laws of the monotonic temporal decay of each of the polarization moments ρ_q^κ separately that are characteristic of random isotropic collisions are replaced by complicated multiexponential laws that describe the decay and mutual conversions of the polarization moments. As a result, the polarization of the light emitted by the atoms after their pulsed excitation can decay in a nonmonotonic way in time, going through maxima and minima and even damped oscillations of the nature of beats.

We now consider polarization beats during laser excitation of the atoms. A characteristic feature of these beats is that the amplitudes and shape of the beat signals depend on the laser frequency, which determines the degree of anisotropy of the distribution of relative velocities of the colliding particles.

The lowest angular momentum of an isolated atomic state for which polarization beats are possible is $J=3/2$. In the coupling of polarization moments of different ranks κ in the course of the anisotropic collisional relaxation, the projections q onto the laser beam are conserved. For longitudinal components of the polarization moments ($q=0$), the parity of their ranks κ is conserved. The orientation ($\kappa=1$) can thus exhibit beats only beginning at $J=3/2$, at which point the quantities ρ_0^1 and ρ_0^3 , i.e., the longitudinal components of the ordinary and octupole orientations, become coupled. A similar result is found for the transverse alignment $\rho_{\pm 2}^2$, which may become coupled with a component of the octupole orientation, $\rho_{\pm 2}^3$, which in turn exists beginning at $J=3/2$. The longitudinal alignment of the angular moment ρ_0^2 along the laser beam, on the other hand, is not coupled with ρ_0^0 for an isolated atomic level (because of the conservation of the total population during collisions), but it may become coupled with the hexadecapole alignment ρ_0^4 , which exists beginning at $J=2$.

To illustrate the situation we consider the example of the polarization beat signal corresponding to mutual conversion of the alignment and the octupole orientation of the angular momenta of the excited atoms. We assume that a laser pulse polarized along the y axis excites the electronic transition $J_0=1/2 \rightarrow J=3/2$ in the A atoms. At the time of excitation, the A atoms then acquire the following polarization moments: a population $\rho_0^0=2/\sqrt{6}$ and longitudinal and transverse (with respect to the laser beam) alignments $\rho_0^0=1/6$ and $\rho_{\pm 2}^2=1/2$. (The values of the polarization moments are given in an arbitrary normaliza-

tion, which depends on the intensity of the exciting light.) The polarization beat mechanism is governed in this case by the coupling of the polarization moments $\rho_{\pm 2}^2$ and $\rho_{\pm 2}^3$, whose time evolution is described by the following equations, in which anisotropic collisions and radiative decay are taken into account:

$$\begin{aligned}\dot{\rho}_{\pm 2}^2 &= -(\Gamma_0 + a)\rho_{\pm 2}^2 + ib\rho_{\pm 2}^3, \\ \dot{\rho}_{\pm 2}^3 &= ib\rho_{\pm 2}^2 - (\Gamma_0 + c)\rho_{\pm 2}^3.\end{aligned}\quad (44)$$

The quantities a , b , and c are real. They are related to the density of the background gas and to the rate constants of the anisotropic collisional relaxation of the polarization moments:

$$a = n_B \langle v\sigma_2^{22} \rangle, \quad b = in_B \langle v\sigma_2^{23} \rangle, \quad c = n_B \langle v\sigma_2^{33} \rangle. \quad (45)$$

The system of differential equations in (44) should be solved under the initial conditions $\rho_{\pm 2}^2=1/2$, $\rho_{\pm 2}^3=0$. As a result we find the following two-exponential law for the transverse alignment as a function of time:

$$\begin{aligned}\rho_{\pm 2}^2(t) &= [(a - \gamma_2)\exp(-\gamma_1 t) + (\gamma_1 - a)\exp \\ &(-\gamma_2 t)] / 2(\gamma_1 - \gamma_2).\end{aligned}\quad (46)$$

The exponents γ_1 and γ_2 , which determine the effect of collisions on the transverse alignment, are given by

$$\gamma_{1,2} = \frac{1}{2} [a + c \pm \sqrt{(a - c)^2 - 4b^2}]. \quad (47)$$

The expression in the radical can be either positive or negative. If it is positive, the quantities γ_1 and γ_2 are purely real, and the time dependence (46) of the transverse alignment is a linear combination of two exponentially damped functions. If it is instead negative, the quantities γ_1 and γ_2 are complex, and the time dependence of the alignment reduces to oscillations at the frequency

$$\omega = \frac{1}{2} \sqrt{4b^2 - (a - c)^2}, \quad (48)$$

which decay by the exponential law $\exp[-(\gamma + \Gamma_0)t]$, where

$$\gamma = -(a + c)/2. \quad (49)$$

The quantities a , b , and c in (45) and, along with them, the quantities $\gamma_{1,2}$ in (47), ω in (48), and γ in (49), are proportional to the density of the background gas B. The rate at which the polarization beats grow and decay in time is therefore proportional to the pressure of the background gas. In this regard, the polarization beats differ from the quantum beats^{55,56} which arise during excitation of a group of atomic levels whose frequencies are determined by the differences between the individual energy levels in this group.

Calculations show that beat frequency (48) is usually small in comparison with the damping rate (49). In practice, therefore, only the first half-wave of the damped polarization oscillations will be seen, and the polarization signals will join smoothly as the expression in the radical in (47) crosses zero. The time evolution of transverse alignment (46) will be nonmonotonic in this case for both signs

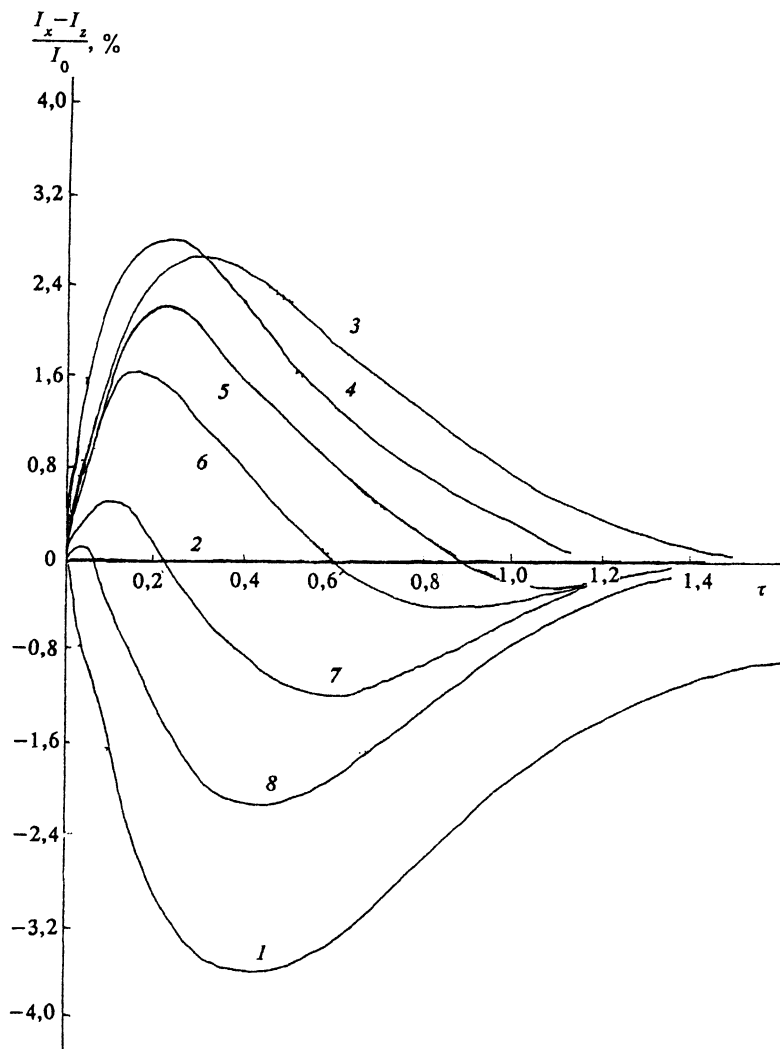


FIG. 8. Polarization beat signals for potassium atoms excited by a laser pulse into the $4p\ ^2P_{3/2}$ state in a xenon atmosphere for various values of the parameter giving the detuning of the laser frequency from the center of the Doppler absorption line, $4s\ ^2S_{1/2}-4p\ ^2P_{3/2}$, $\zeta=0$; 2—0.535; 3—1.00; 4—1.50; 5—1.75; 6—2.00; 7—2.50; 8—3.00.

of the expression in the radical. This circumstance will be manifested in a corresponding time dependence for the intensity differences ($I_x - I_z$) between the light linearly polarized perpendicular to the laser beam (and to the polarization of the exciting light) and the light polarized along the beam. Constructing the ratio of this intensity difference to the total intensity of the emitted light, we find

$$\frac{I_x(t) - I_z(t)}{I(t)} = \frac{\sqrt{6}\rho_0^2(t) - 2\rho_2^2(t)}{2\sqrt{6}\rho_0^0(t)}. \quad (50)$$

At the time of the pulsed excitation of the atoms ($t=0$) the numerator of the fraction on the right-hand side is zero, and there is no polarization beat signal. However, because of the simple one-exponential decay of the longitudinal alignment component $\rho_0^2(t)$ and the two-exponential law in (46) for the relaxation of the transverse alignment $\rho_2^2(t)$, the "equilibrium" between the two terms in the numerator of the fraction will be disrupted at $t > 0$, and a nonzero signal (5) will appear. The nonmonotonic time evolution of this signal reflects the "polarization beats."

We have calculated the polarization beat signal in (50) for potassium atoms (in the $4p\ ^2P_{3/2}$ state) excited by a laser pulse in a xenon atmosphere for various values of the

parameter ζ in (7). This parameter determined the detuning of the laser frequency from the center of the Doppler line. The polarization beams are determined in this case by the mutual conversion of the polarization moments of ranks $\kappa=2$ and $\kappa=3$, i.e., by the rate constant $\langle v\sigma_2^{23} \rangle$, which depends on the dynamic multipole moments S_2 and S_4 of the velocity distribution (Table I). The numerical calculations showed that this rate constant and, along with it, the quantity b in (45) vanish at $\zeta=0.535$. At this value of ζ there are no polarization beats. As ζ deviates from 0.535, the beat signal is nonzero; it has opposite signs at the center of the Doppler line ($\zeta=0$) and at its wing ($\zeta > 0.535$). With increasing value of the parameter ζ (i.e., far out on the wing of the Doppler profile), the alternating nature of the polarization beat signal becomes progressively more obvious. This trend is accompanied by a decrease in the area under its positive "half-wave" and an increase in its negative half-wave. The maximum calculated value of the polarization beam signal in (50) reaches 3–4% under these conditions. Figure 8 shows the results of these calculations in graphical form. The ratio of the difference between the intensity of the light polarized linearly along the x and z axes to the total intensity of the emitted light is plotted along the ordinate. The dimensionless time

$\tau = n_B |\Delta C / \hbar|^{2/5} [2(M_A + M_B) kT / M_A M_B]^{3/10} t$ is plotted along the abscissa, where T is the temperature, n_B is the number density of inert gas B, M_A and M_B are the masses of the atoms of the gas under study and of the background gas, ΔC is the splitting of the excited $^2P_{3/2}$ level of the K atom due to the dispersive K–Xe interaction, and t is the time.

This calculation shows that the light polarization beats during laser excitation are quite accessible to experimental observation and that they could be used to measure the rate constants for the mutual conversion of the polarization moments of various ranks under conditions of anisotropic collisions.

10. CONCLUSION

The results found here show that the laser-excitation method makes it possible to study all the characteristic features of the anisotropic collisional relaxation of the atomic polarization moments, including the mutual conversion of the alignment and orientation of atomic angular momenta, the creation of an alignment of angular momenta from the atomic level populations, the effect of the degree of alignment of the atomic states and the laser frequency on the rates of the collision-induced transitions between atomic levels, and the polarization beat processes. While surpassed by the atomic-beam method in terms of the magnitude of the degree of anisotropy of the velocity distribution function, the laser-excitation method has the advantage of simplicity in practical implementation and the flexibility of being able to continuously adjust the degree of anisotropy of the relaxation by tuning the laser frequency. There are substantial opportunities for raising the degree of anisotropy of the relaxation by switching to excitation further out on the wing of the Doppler profile and by using background gases as heavy as possible (perhaps polyatomic gases). Some interesting possibilities are also raised by the technique of a composite excitation of the atoms by two or more lasers. This approach would permit even greater flexibility in manipulating the degree of anisotropy of the relaxation and the polarization characteristics of the light. The method of laser excitation of atoms in the gas phase is thus a promising method for studying the diverse processes of anisotropic collisional relaxation of atomic polarization moments and the polarization characteristics of the light which they determine.

¹ M. I. D'yakonov, Zh. Eksp. Teor. Fiz. **47**, 2213 (1964) [Sov. Phys. JETP **20**, 1484 (1964)].

² M. I. D'yakonov and V. I. Perel', Zh. Eksp. Teor. Fiz. **48**, 345 (1965) [Sov. Phys. JETP **21**, 227 (1965)].

³ A. Omont, J. Phys. (Paris) **26**, 26 (1965).

⁴ A. Omont, Progr. Quantum Electron. **5**, 69 (1977).

⁵ K. Blum, *Density Matrix Theory and Applications*, Plenum, New York, 1981.

⁶ S. A. Kazantsev, N. Ya. Polynovskaya, L. N. Pyatnitskiĭ, and S. A. Edel'man, Usp. Fiz. Nauk **156**, 3 (1988) [Sov. Phys. Usp. **31**, 785 (1988)].

⁷ E. B. Aleksandrov, G. I. Khvostenko, and M. P. Chaĭka, *Interference of Atomic States*, Nauka, Moscow, 1991.

⁸ V. N. Rebane, *V Internat. Conf. Physics Electronic and Atomic Collisions. Abstracts*, Leningrad, 1967, p. 229.

⁹ V. N. Rebane, Opt. Spektrosk. **24**, 309 (1968).

¹⁰ M. Lombardi, C. R. Acad. Sci. **265**, 191 (1967).

¹¹ M. I. D'yakonov and V. I. Perel, *Sixth Internat. Conf. Atomic Physics. Proceedings*, Riga, 1978, p. 410.

¹² A. P. Yutsis and A. A. Bantszaitis, *Angular Momentum Theory in Quantum Mechanics*, Mintis, Vil'nyus, 1965.

¹³ E. Chamoun, M. Lombardi, M. Carre, and M. L. Gaillard, J. Phys. (Paris) **38**, 591 (1977).

¹⁴ T. Manabe, T. Yabuzaki, and T. Ogawa, Phys. Rev. A **20**, 1946 (1979).

¹⁵ T. Manabe, T. Yabuzaki, and T. Ogawa, Phys. Rev. Lett. **46**, 637 (1981).

¹⁶ A. G. Petrashen', V. N. Rebane, and T. K. Rebane, Opt. Spektrosk. **57**, 963 (1984) [Opt. Spectrosc. (USSR) **57**, 588 (1984)].

¹⁷ N. G. Lukomskii, V. A. Polishuk, and M. P. Chaĭka, Opt. Spektrosk. **58**, 474 (1985) [Opt. Spectrosc. (USSR) **58**, 284 (1985)]; **59**, 1008 (1985) [**59**, 606 (1985)].

¹⁸ A. G. Petrashen' and V. N. Rebane, Opt. Spektrosk. **60**, 696 (1986) [Opt. Spectrosc. (USSR) **60**, 425 (1986)].

¹⁹ E. I. Dashevskaya and E. E. Nikitin, Opt. Spektrosk. **62**, 742 (1987) [Opt. Spectrosc. (USSR) **62**, 442 (1987)].

²⁰ H. Avci and H. P. Neitzke, J. Phys. B **22**, 495 (1989).

²¹ A. G. Petrashen', V. N. Rebane, and T. K. Rebane, Opt. Spektrosk. **69**, 259 (1990) [Opt. Spectrosc. (USSR) **69**, 157 (1990)].

²² M. Elbel, M. Simon, and T. Strauss, Ann. Phys. (Leipzig) **47**, 467 (1990).

²³ M. Elbel, H. Hühnermann, T. Meier, and W. B. Schneider, Z. Phys. A **275**, 339 (1975).

²⁴ A. G. Petrashen', V. N. Rebane, and T. K. Rebane, Opt. Spektrosk. **55**, 819 (1983) [Opt. Spectrosc. (USSR) **55**, 492 (1983)].

²⁵ K. J. Nieuwesteeng, T. J. Hollander, C. Th. Alkemade, J. Quant. Spectros. Radiat. Transfer **30**, 97 (1983).

²⁶ A. G. Petrashen', V. N. Rebane, and T. K. Rebane, Zh. Eksp. Teor. Fiz. **87**, 147 (1984) [Sov. Phys. JETP **60**, 84 (1984)].

²⁷ E. I. Dashevskaya, E. E. Nikitin, and S. Ya. Umanskiĭ, Khim. Fiz. **3**, 627 (1984).

²⁸ A. G. Petrashen', V. N. Rebane, and T. K. Rebane, Opt. Spektrosk. **58**, 785 (1985) [Opt. Spectrosc. (USSR) **58**, 481 (1985)].

²⁹ S. A. Kazantsev, A. G. Petrashen', N. T. Polezhaeva, V. N. Rebane, and T. K. Rebane, Pis'ma Zh. Eksp. Teor. Fiz. **45**, 15 (1987) [JETP Lett. **45**, 17 (1987)].

³⁰ S. A. Kazantsev, N. T. Polezhaeva, and V. N. Rebane, Opt. Spektrosk. **63**, 27 (1987) [Opt. Spectrosc. (USSR) **63**, 15 (1987)].

³¹ S. A. Kazantsev, A. G. Petrashen', N. T. Polezhaeva, V. N. Rebane, and T. K. Rebane, *Nineteenth European Group Atomic Spectroscopy Conf., Abstracts*, 11E, Dublin, 1987, p. 3–12.

³² A. G. Petrashen', V. N. Rebane, and T. K. Rebane, Opt. Spektrosk. **65**, 811 (1988) [Opt. Spectrosc. (USSR) **65**, 479 (1988)].

³³ N. Homaïdan, E. Chamoun, and R. Abou-Chacra, Czech. J. Phys. B **28**, 634 (1978).

³⁴ V. N. Rebane and T. K. Rebane, Opt. Spektrosk. **59**, 771 (1985) [Opt. Spectrosc. (USSR) **59**, 465 (1985)].

³⁵ R. L. Robinson, L. J. Kovalenko, and S. R. Leone, Phys. Rev. Lett. **64**, 388 (1990).

³⁶ L. Hiewel, J. Maer, and H. Pauly, J. Chem. Phys. **76**, 4961 (1982).

³⁷ V. N. Rebane and T. K. Rebane, Opt. Spektrosk. **54**, 761 (1983) [Opt. Spectrosc. (USSR) **54**, 451 (1983)].

³⁸ M. O. Hale, J. V. Hertel, and S. R. Leone, Phys. Rev. Lett. **53**, 2296 (1984).

³⁹ W. Bussert, D. Neuschafer, and S. Leone, J. Chem. Phys. **87**, 3833 (1987).

⁴⁰ L. J. Kovalenko, S. R. Leone, and J. B. Delos, J. Chem. Phys. **91**, 6948 (1989).

⁴¹ G. C. Schatz, L. J. Kovalenko, and S. R. Leone, J. Chem. Phys. **91**, 9661 (1989).

⁴² L. J. Kovalenko, J. B. Delos, and S. R. Leone, *Sixteenth International Conf. Physics Electron. Atomic Collisions, Abstracts*, New York, 1989, p. 704.

⁴³ A. L. Zagrebina, Zh. Eksp. Teor. Fiz. **97**, 114 (1990).

⁴⁴ A. L. Zagrebina, Opt. Spektrosk. **69**, 278 (1990) [Opt. Spectrosc. (USSR) **69**, 167 (1990)].

⁴⁵ A. G. Petrashen', V. N. Rebane, and T. K. Rebane, Opt. Spektrosk. **72**, 280 (1992) [Opt. Spectrosc. (USSR) **72**, 152 (1992)].

⁴⁶ V. N. Rebane and T. K. Rebane, Opt. Spektrosk. **66**, 763 (1989) [Opt. Spectrosc. (USSR) **66**, 446 (1989)].

⁴⁷ A. Yu. Artem'ev, Teor. Mat. Fiz. **87**, 34 (1991).

- ⁴⁸ A. Yu. Artem'ev and O. I. Fisun, *Opt. Spektrosk.* **71**, 21 (1991) [*Opt. Spectrosc. (USSR)* **71**, 11 (1991)].
- ⁴⁹ A. G. Petrashen', V. N. Rebane, and T. K. Rebane, *Opt. Spektrosk.* **69**, 17 (1990) [*Opt. Spectrosc. (USSR)* **69**, 10 (1990)].
- ⁵⁰ A. G. Petrashen', V. N. Rebane, and T. K. Rebane, *Opt. Spektrosk.* **61**, 214 (1986) [*Opt. Spectrosc. (USSR)* **61**, 138 (1986)].
- ⁵¹ A. G. Petrashen', V. N. Rebane, and T. K. Rebane, *Zh. Eksp. Teor. Fiz.* **94** (11), 46 (1988) [*Sov. Phys. JETP* **67**, 2202 (1988)].
- ⁵² M. Lombardi, These, Universite Grenoble, 1969.
- ⁵³ A. I. Okunevich and V. I. Perel', *Zh. Eksp. Teor. Fiz.* **58**, 666 (1970) [*Sov. Phys. JETP* **31**, 356 (1970)].
- ⁵⁴ B. Storr and M. Baumann, *Z. Phys. D* **9**, 171 (1988).
- ⁵⁵ E. B. Aleksandrov, *Opt. Spektrosk.* **14**, 436 (1963).
- ⁵⁶ E. B. Aleksandrov, *Usp. Fiz. Nauk* **108**, 595 (1972) [*Sov. Phys. Usp.* **15**, 831 (1972)].

Translated by D. Parsons